NASA Technical Paper 2970

January 1990

Heat Treatment Study of the SiC/Ti-15-3 Composite System

Bradley A. Lerch,
Timothy P. Gabb,
and Rebecca A. MacKay

NASA

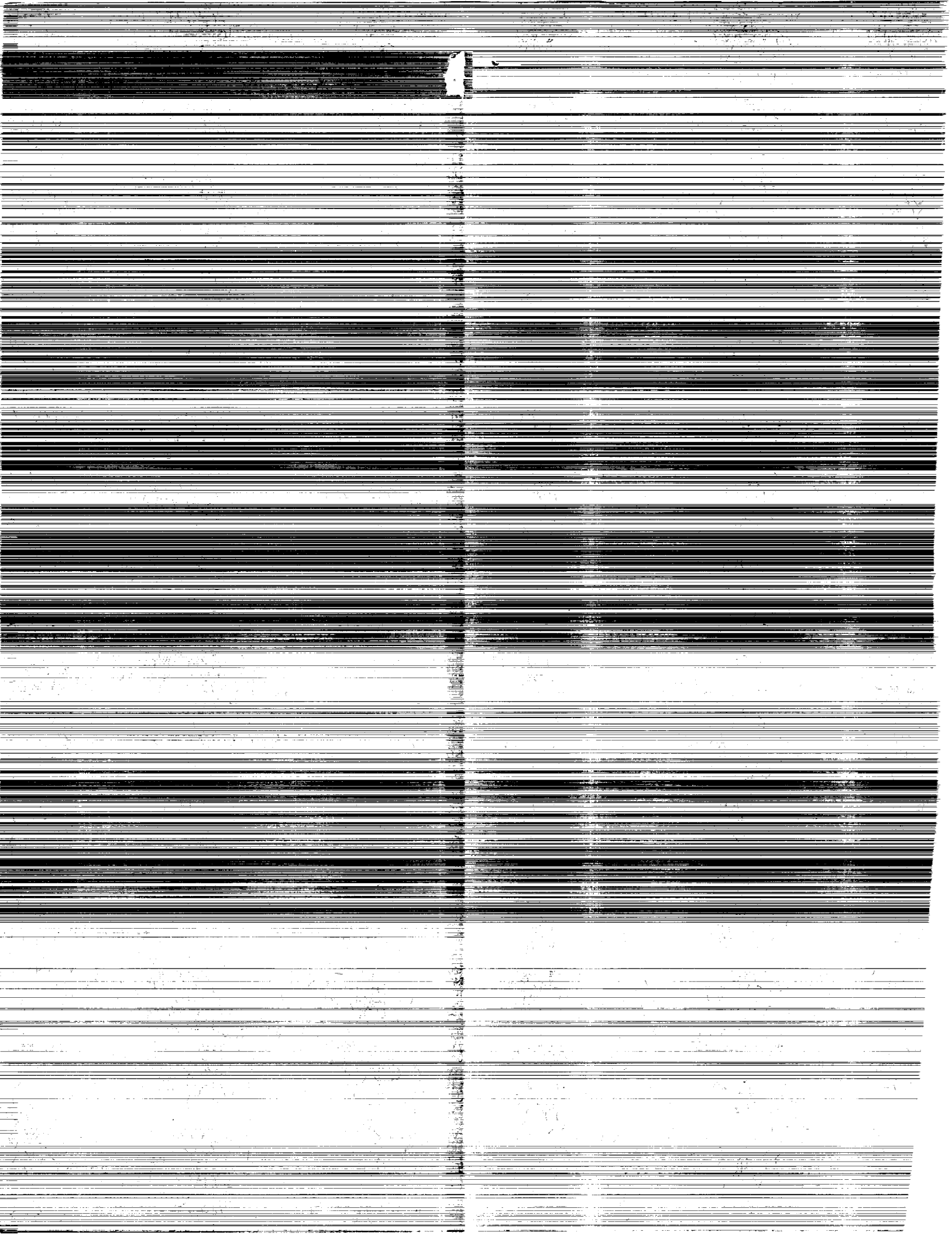

NASA
Technical
Paper
2970

1990

Heat Treatment Study of the SiC/Ti-15-3 Composite System

Bradley A. Lerch,
Timothy P. Gabb,
and Rebecca A. MacKay
Lewis Research Center
Cleveland, Ohio

National Aeronautics and
Space Administration
Office of Management
Scientific and Technical
Information Division

Summary

The oxidation and aging behaviors of a continuous fiber SiC/Ti-15V-3Cr-3Sn-3Al composite (SiC/Ti-15-3) were investigated. The aging characteristics of the composite were compared with those of the unreinforced Ti-15-3 matrix material, which was processed in the same manner as the composite. Various age-hardened conditions of both the unreinforced matrix and the composite were evaluated by using optical microscopy, hardness measurements, and room-temperature tensile tests (unreinforced matrix only).

The Ti-15-3 material formed a thick surface oxide at temperatures at or above 550 °C when heat treated in air. The in situ composite matrix was softer than the unreinforced matrix for equivalent aging conditions. Both materials hardened to a maximum, then softened during overaging. The temperature at which peak aging occurred was ~450 °C for both the in situ composite matrix and the unreinforced matrix. The room-temperature elastic modulus and ultimate tensile strength of the unreinforced matrix varied as a function of aging treatment and paralleled the hardness behavior. The modulus and tensile strength showed little response to aging up to temperatures of 300 °C; however, these properties increased after aging at 550 °C. Aging at temperatures above 550 °C resulted in a decrease in the modulus and tensile strength. The failure strain was a function of the precipitation state and of the amount of oxidation resulting from the heat treatment. Aging in air at the higher temperatures (>550 °C) caused the formation of a thick oxide layer and reduced the ductility. Aging in vacuum at these temperatures resulted in significantly higher ductilities. Long-term exposures at 700 °C caused the formation of a large, grain boundary α phase which reduced the ductility, even though the specimens were heat treated in vacuum.

Introduction

The composite material SiC/Ti-15V-3Cr-3Sn-3Al (henceforth referred to as SiC/Ti-15-3) is currently being investigated for use in airframes and in propulsion systems. To provide reliable design data, evaluation of the composite's performance and the performance of the constituents will be needed. Some work has been done on the aging characteristics and subsequent mechanical properties of rolled Ti-15-3 sheet (refs. 1 to 6). Okada et al. (ref. 6) have documented the microstructures and room-temperature tensile properties for specimens aged between 2 and 100 hr at temperatures of 300, 500, and 600 °C. Aging at 300 °C for less than ~30 hr resulted in no change in properties compared with the solution-treated state. Longer aging led to a rapid increase in tensile strength. After 100 hr at 300 °C, the tensile strength was approximately twice that observed for the solution-treated specimens. This strength increase was coupled with a loss in ductility; there was no observable tensile ductility after a 100-hr age. The brittle behavior was suggested to result from the localization of slip due to a high volume fraction of fine α-precipitates. Planar slip caused large offsets on the surface of the specimen and resulted in crack nucleation. A reasonable ductility (>8 percent) was maintained during aging at 500 and 600 °C for all aging times investigated. Aging for 5 hr at 500 °C resulted in a large increase in the tensile strength. No further changes in the strength were observed for longer aging times. Little increase in the strength was noticed after aging at 600 °C for times up to 100 hr.

The investigation of Okada et al. (ref. 6) has shown that the properties of Ti-15-3 can change drastically as a function of temperature. The most severe aging can reduce the ductility to zero, a situation to be avoided with the monolithic material. Whether or not the composite will become embrittled is at this time unknown, but avoiding this particular precipitate state would be prudent. It is also not clear if the composite will exhibit the same aging characteristics as the unreinforced matrix. The in situ composite matrix could contain chemical impurities from the reinforcements which may alter the aging characteristics. The composite also contains a residual stress state due to the differences in the coefficients of thermal expansion between the fiber and the matrix. This stress state may also affect aging.

Thus, in the present study, to compare the aging characteristics, a composite consisting of Ti-15-3 reinforced with SCS-6 (SiC) fibers was examined together with unreinforced Ti-15-3 material which was processed in the same manner as the composite. Emphasis was placed on the examination of microstructural and property changes as a function of aging. This study makes no attempt to explain hardening mechanisms in this material, but simply documents similarities and differences in the microstructure of the unreinforced matrix and the composite matrix as a function of aging. The aging treatments were conducted over a wide temperature range, which included temperatures higher than those normally recommended for the aging and use of monolithic Ti-15-3.

This was justified, since the composite may be able to withstand higher service temperatures because of the reinforcement. To assess the stability of the microstructure, several duplex heat treatments and long-term exposures were employed. These results, together with oxidation data, may assist in determining a maximum use temperature for the composite.

Material and Experimental Procedures

The composite material was fabricated from alternating plies of Ti-15-3 foils and continuous SCS-6 (SiC) fibers. Unidirectional $[0°]_8$ composite sheets were consolidated at elevated temperatures in a proprietary process. Coupons (~1.3 by 1.3 cm by plate thickness) of the unreinforced matrix (0.5 cm thick) and the composite (0.2 cm thick) were simultaneously aged at temperatures between 300 and 700 °C for periods of 24 hr. Other thermal treatments were occasionally used and will be indicated where appropriate. Heat treatments were performed in a variety of atmospheres, including air, argon, and vacuum (10^{-2} or 10^{-7} torr), in order to evaluate any possible effects of oxygen. The materials were then sectioned, prepared by standard metallographic techniques, and etched with a solution of 20 ml H_2O_2 added to 120 ml distilled water and 12 g NaOH at 80 °C. The samples were examined with an optical microscope. The various heat treatments used for the unreinforced matrix and composite are given in tables I and II, respectively. Also indicated in the tables are the figure numbers for those heat treatments for which micrographs are included in this report.

A minimum of six Vickers hardness indentations were made with a 200-g load on each matrix and composite coupon. These measurements were performed on interior grains of the matrix to avoid specimen surface effects and any possible surface oxidation. Furthermore, each indentation was placed in the center of the interior grain and away from fibers in an attempt to obtain a true hardness measurement of the matrix.

Tensile specimens (2.54 cm gauge length and 0.32 cm gauge diameter) of the matrix were heat treated under some of the same conditions as the coupons. These were tested at room temperature at a constant displacement rate of 4.3×10^{-3} cm/sec, which yielded a total strain rate of 3×10^{-3} sec^{-1}. Table I also lists for which heat treatments tensile tests were performed and whether tensile specimens were heat treated in a vacuum prior to testing.

TABLE I.—HEAT TREATMENT CONDITIONS OF UNREINFORCED MATRIX

Heat treatment conditions, °C/hr	Figure	Tensile test[a]
As-received	2(a), 14(a) and (b)	X
300/24	----	X
300/24 + 565/24	----	----
300/100	----	----
450/24	15(a)	----
500/24	----	----
540/24	----	----
565/24	----	X
593/24	----	X
593/24 + 550/24	----	X
600/24	16(a)	X
620/24	----	----
650/24	----	X_{vac}
680/24	----	X_{vac}
700/24	3(a), 17(a) and (b)	X,X_{vac}
700/24 + 600/165	18(a) and (b)	X_{vac}
700/168	4(a), 19(a) and (b)	X_{vac}
788/0.25	20(a) and (b)	----
788/0.25 + 300/24	21(a) and (b)	----
788/0.25 + 400/24	----	----
788/0.25 + 500/24	----	----
788/0.25 + 600/24	----	----
788/0.25 + 700/24	5(a), 22(a) and (b)	----

[a]X indicates tensile tested at room temperature; X_{vac} indicates heat treated in vacuum and tensile tested at room temperature.

TABLE II.—HEAT TREATMENT CONDITIONS OF COMPOSITE

Heat treatment conditions, °C/hr	Figure
As-received	2(b), 14(c) and (d)
300/24	----
300/24 + 565/24	----
300/100	----
450/24	15(b)
500/24	----
565/24	----
600/24	16(b) and (c)
650/24	----
700/24	3(b), 17(c) and (d)
700/24 + 600/165	18(c) and (d)
700/168	4(b), 19(c) and (d)
788/0.25	20(c)
788/0.25 + 300/24	21(c)
788/0.25 + 400/24	----
788/0.25 + 500/24	----
788/0.25 + 600/24	----
788/0.25 + 700/24	5(b), 22(c) and (d)

Results and Discussion

Oxide Thickness

The surface oxide thickness was examined as a function of aging temperature. Six measurements were obtained for each

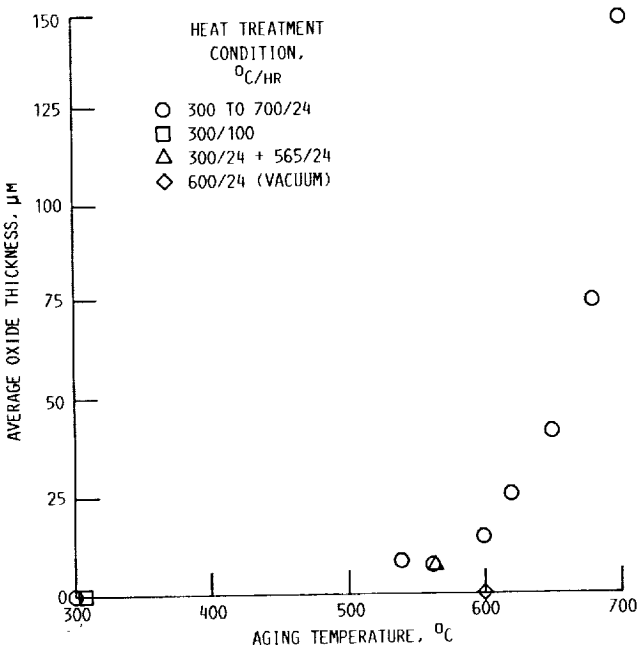

Figure 1.—Surface oxide thickness as function of aging temperature for Ti–15–3 unreinforced matrix coupons (all specimens exposed in air unless otherwise noted).

matrix coupon, and these were averaged and plotted as a function of the aging temperature (fig. 1). The aging treatments were all performed in air, except for the treatment conducted in a vacuum at 600 °C for 24 hr. The oxide was very adherent, except for the very thickest layers, which formed after aging above 650 °C; thus, spalling is not believed to have influenced the measurements. Figure 1 shows that there was no oxide formation for aging temperatures at or below 300 °C, and that there was a minimal increase in the oxide thickness with increasing temperature from 300 to ~550 °C. However, above 550 °C, the oxide thickness greatly increased with temperature. The coupon subjected to the duplex heat treatment had an oxide thickness corresponding to that of the higher exposure temperature, as shown in figure 1. No visible oxide was observed for the coupon exposed at 600 °C in a vacuum at 10^{-2} torr. Coupons which were heat treated at intermediate temperatures in argon (not high purity, not gettered) exhibited oxide thicknesses similar to those heat treated in air. Composite coupons also had oxide thicknesses identical to the unreinforced matrix.

Figure 1 suggests that reinforced Ti–15–3 composites exposed to temperatures greater than 550 °C must be protected from the environment. It should be emphasized that these results represent gross surface oxidation and do not reflect the amount of oxygen which may have penetrated into the matrix. Diffusion of oxygen into some Ti-alloys can be quite significant (ref. 7). In addition, these results do not address the diffusion of oxygen along the fiber/matrix interface.

Microstructures

Etched coupons were examined by optical microscopy, and only selected micrographs (as indicated in table I) are shown in the figures. Micrographs for both the unreinforced matrix and composite for most of the aging conditions are presented in the appendix for completeness. There was no observable change in the thickness of the reaction zone between the fiber and the matrix for any of the heat treatment conditions used in this study.

The as-received matrix microstructure contained large needles of α-Ti as well as areas of a dark, blotchy phase in a matrix of β. Both the α-phase and the dark phase were concentrated primarily at grain and laminae boundaries (fig. 2(a)). The dark phase is believed to be the β'-phase, which is a solute lean, coherent, body-centered cubic (bcc) phase. Standardless x-ray analysis indicated that these areas were lower in all the alloying elements than the β-matrix (ref. 8). The β'-phase has been observed in several β-Ti alloys (refs. 9 to 11) and tends to form where precipitation of the α-phase is sluggish (ref. 9). A similar precipitate structure was observed in the composite, although a precipitate lean zone was evident around the fibers (fig. 2(b)).

After aging the unreinforced matrix and composite coupons at 700 °C/24 hr, the dark β'-phase was replaced by large needles of α-Ti (fig. 3(a)). The α-phase has been identified in conventionally produced Ti–15–3 and is the primary hardening phase (refs. 5, 6, and 12) of the matrix. Large α-particles were present on the grain and laminae boundaries in both the unreinforced matrix and composite coupons. A small precipitate lean zone was observed next to some of the grain boundaries in both the unreinforced matrix and the composite. The precipitate lean zone surrounding the fibers in the composite was still evident (fig. 3(b)). This heat treatment of 700 °C/24 hr produced an overaged structure, as will be shown by the results of the hardness and tensile tests.

After aging at 700 °C/168 hr, the α-phase had coarsened considerably (fig. 4). The most prominent features of this structure are the large α-particles, located at grain and laminae boundaries, and the neighboring precipitate lean zones. These were present in both the unreinforced matrix (fig. 4(a)) and the composite (fig. 4(b)).

Most of the α-precipitates and any residual β' could be solutioned by using a heat treatment of 788 °C/0.25 hr, followed by a water quench. This is the recommended solution temperature for sheet Ti–15–3 (refs. 1 and 5). Subsequent aging at 700 °C/24 hr yielded precipitate structures in the unreinforced matrix and composite which were unlike the as-received material after aging at 700 °C/24 hr. In this solutioned and aged state, the unreinforced matrix contained fewer, yet larger α-particles. (Compare fig. 5(a) with fig. 3(a).) On the other hand, the composite contained essentially no resolvable α-particles. (Compare fig. 5(b) with fig. 3(b).) Some α-phase was occasionally observed between the fibers where a Ti-wire

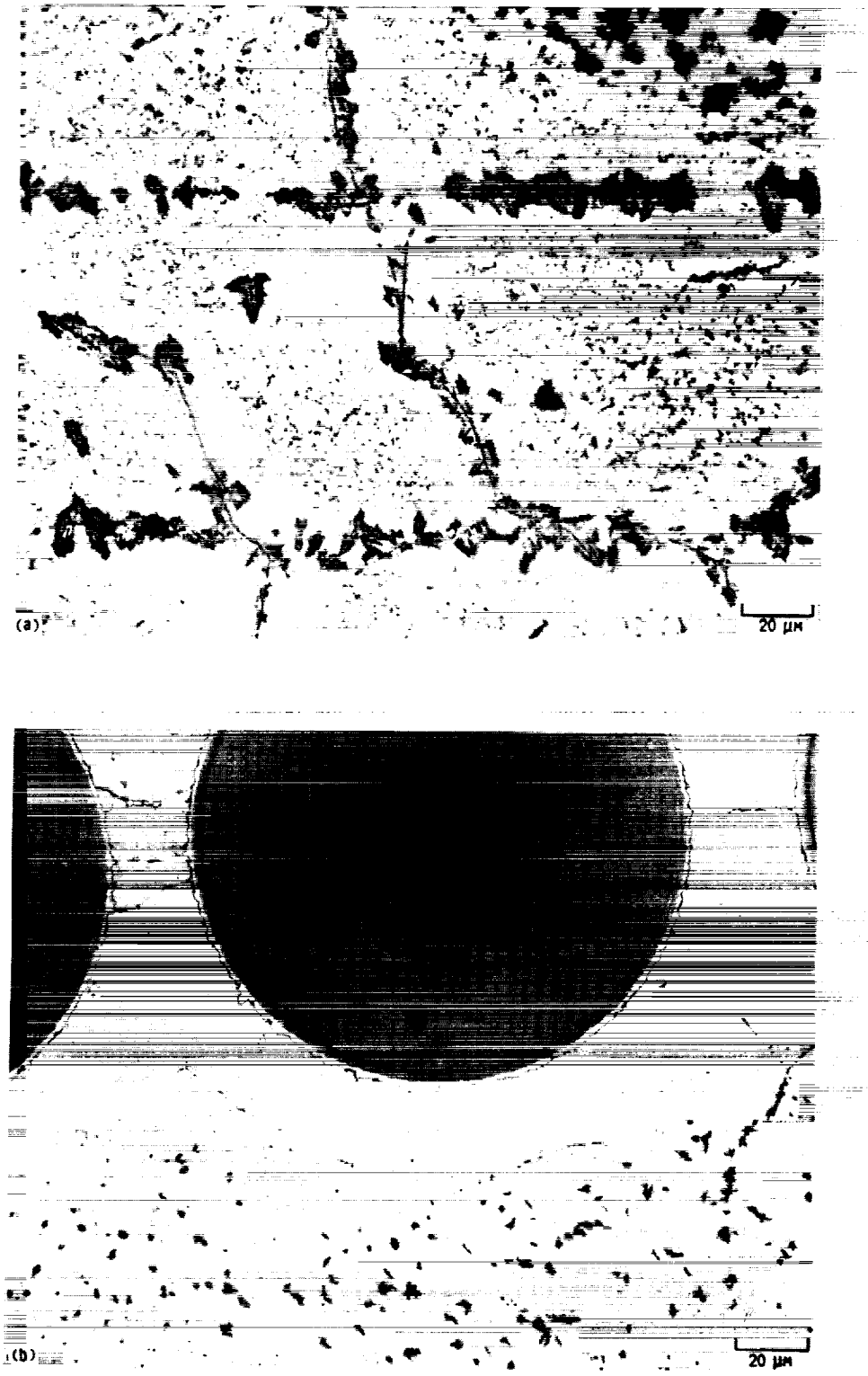

(a) Unreinforced matrix.
(b) Composite matrix.

Figure 2.—As-received materials showing β'-phase (dark phase) in unreinforced matrix and composite matrix. (Note precipitate lean zone surrounding fibers in composite.)

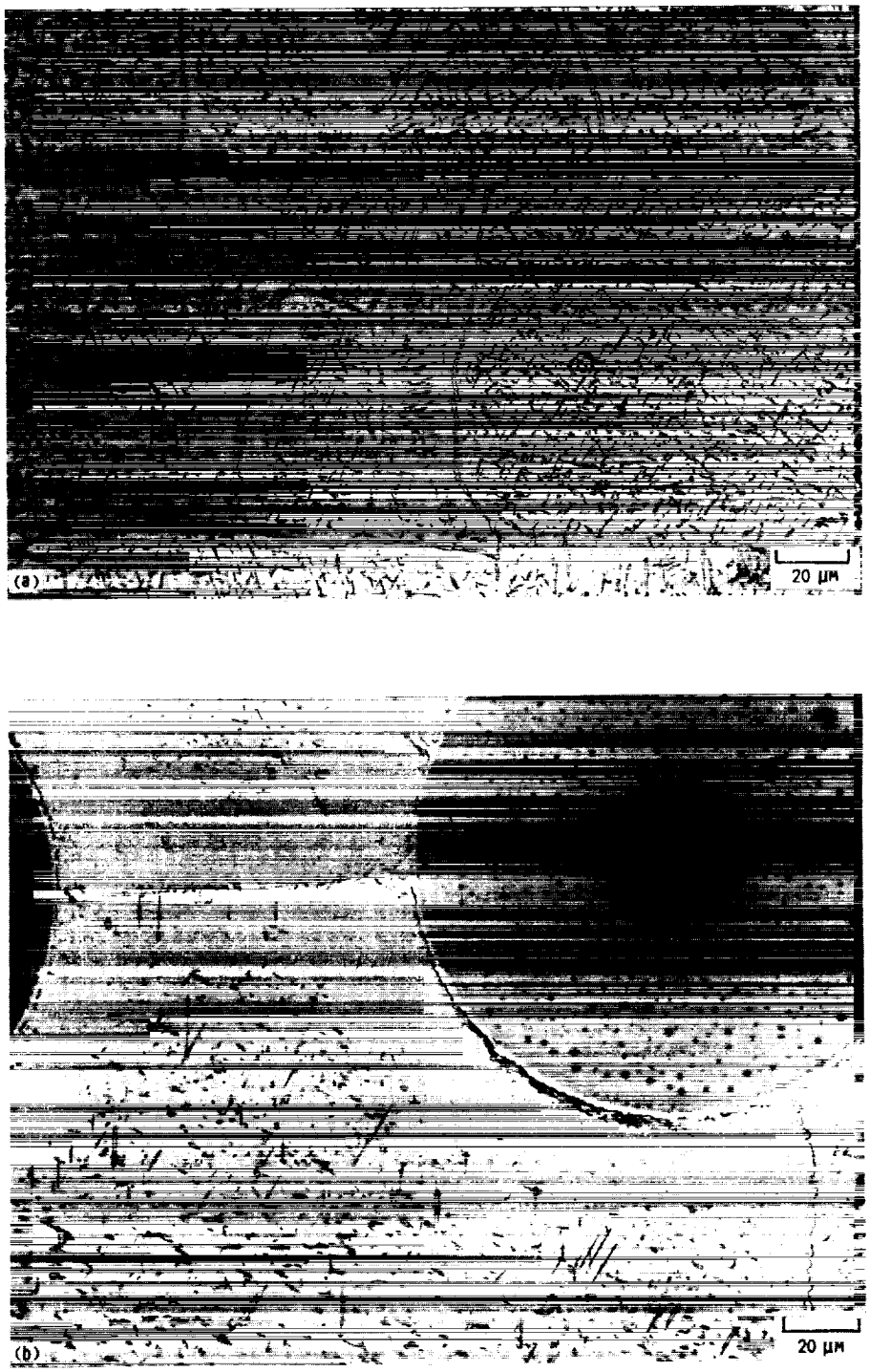

(a) Unreinforced matrix.
(b) Composite matrix.

Figure 3.—Unreinforced matrix and composite matrix after aging for 24 hr at 700 °C (large α-needles apparent in grains).

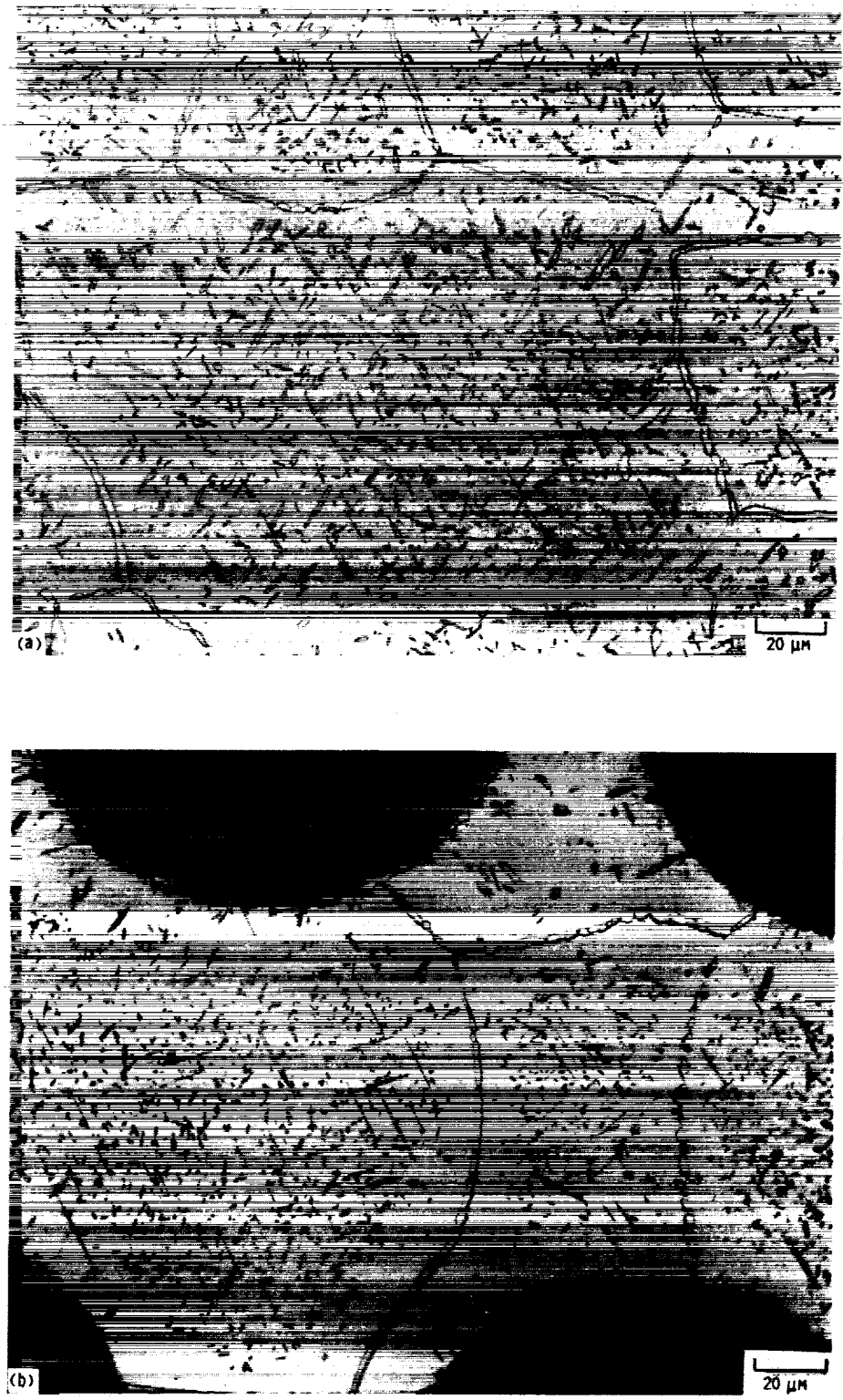

(a) Unreinforced matrix.
(b) Composite matrix.

Figure 4.—Unreinforced matrix and composite matrix after aging for 168 hr at 700 °C. (Note large α-particles at grain and laminae boundaries, surrounded by precipitate free zones.)

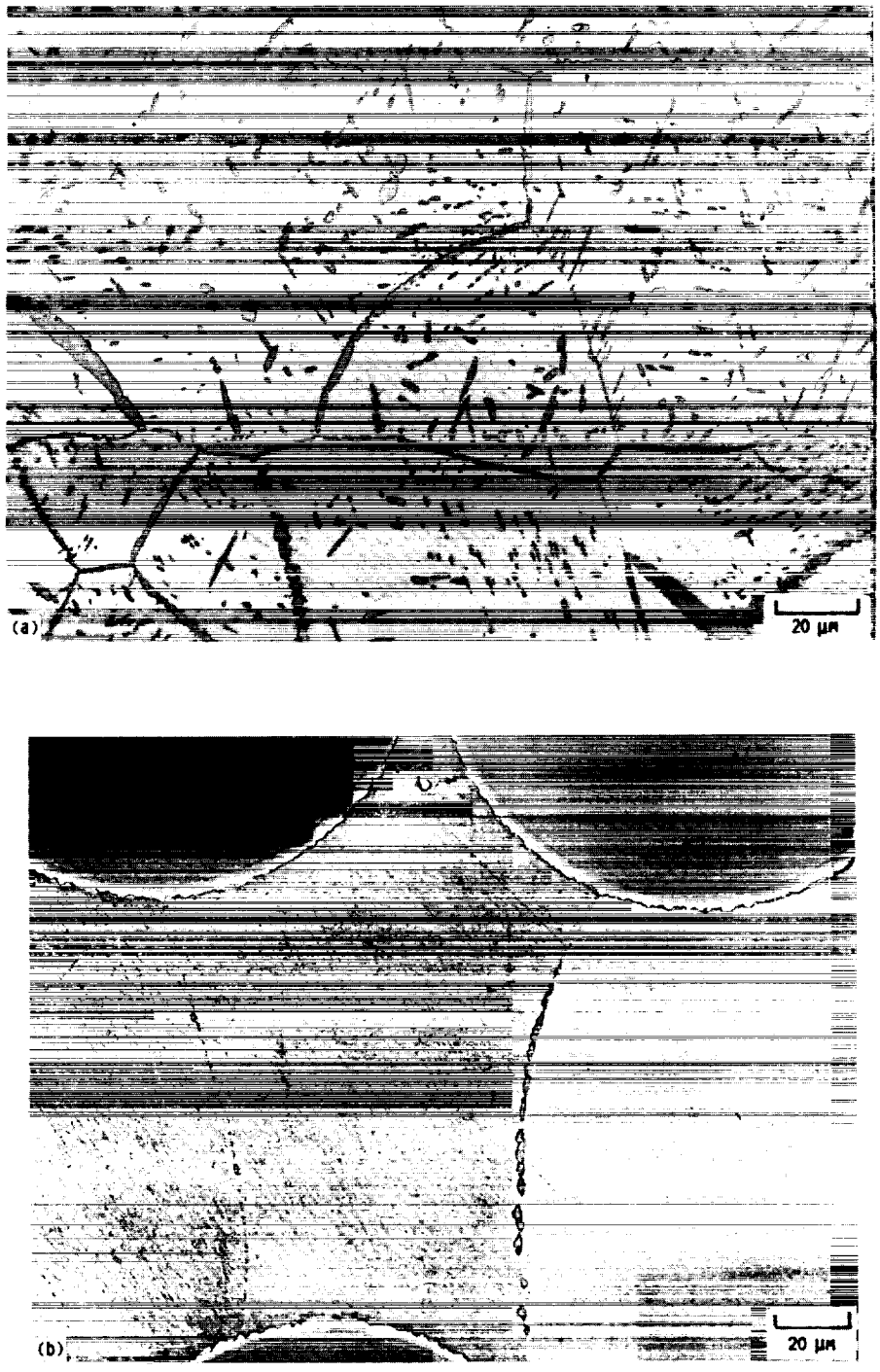

(a) Unreinforced matrix.
(b) Composite matrix.

Figure 5.—Unreinforced matrix and composite matrix after solutioning for 0.25 hr at 788 °C, followed by aging for 24 hr at 700 °C. (Note large α-needles in unreinforced matrix and apparent absense of α in composite matrix.)

had been woven at 5-mm intervals to keep the fibers parallel during consolidation. The Ti-wire created chemical inhomogeneities in these areas (ref. 8). The apparent absence of precipitates in the composite material indicates a difference in aging characteristics between the unreinforced matrix and the composite.

Hardness Measurements

The effects of aging on the hardness of the unreinforced matrix can be observed in figure 6. Vickers hardness (H_v) was measured on all unreinforced matrix coupons, and each data point in figure 6 represents the average of at least six measurements for each specimen. The range of these hardness values per specimen was approximately ± 10 H_v. Most of the specimens were aged for 24 hr from 300 to 700 °C. These data show typical aging behavior with a peak hardness occurring somewhere between 400 and 450 °C for the 24-hr aging time. The heat treatment atmosphere had no apparent effect on hardness, indicating that additional precipitation due to oxygen diffusion into the matrix was minimal for these times and temperatures.

Heat treating at a temperature of 300 °C/24 hr caused a slight increase in hardness over the as-received material even though no apparent differences in the microstructure were observed. The aging kinetics below ~350 °C are very slow for the as-received and aged material. This was evident by the identical hardness for both the 24- and 100-hr aging times at 300 °C and by the low slope of the hardening curve over this temperature range.

One of the concerns for this material is microstructural stability. For instance, would the microstructure change during high-temperature testing, even though the specimen had been previously heat treated? This was addressed by performing duplex heat treatments. The duplex heat treatments of 300 °C/24 hr + 565 °C/24 hr, 593 °C/24 hr + 550 °C/168 hr, and 700 °C/24 hr + 600 °C/165 hr yielded hardness values identical to the simple heat treatments of 565 °C/24 hr, 593 °C/24 hr, and 600 °C/24 hr, respectively. This suggests that, regardless of the initial heat treatment, exposure of the material to a temperature which is different from the heat treating temperature causes some change in the microstructure and, as will be shown by the tensile tests, results in a change in the mechanical properties. Note that the specimen aged at 593 °C/24 hr + 550 °C/168 hr does not follow this trend, probably because the difference between the two temperatures was not large enough to induce a noticeable change during the short aging times involved. The coupon aged at 700 °C/168 hr in a high vacuum had a hardness which was very close to the hardness of the coupon aged for only 24 hr at the same temperature, thus indicating good microstructural stability at this temperature. There was a difference in the amount of grain boundary α (compare fig. 4(a) with fig. 3(a)), as well as in the size and number of discrete α-particles in the matrix, but this had no significant effect on the hardness values.

Solutioning above the β transus had a marked effect on the aging characteristics of the material (fig. 7). The solutioned coupon had the lowest hardness, which suggests that the as-received material was not in the solutioned state. Fine, unresolvable α-precipitates were probably present in the grain interiors in the as-received material and increased the hardness over that of the solutioned material. The β'-phase may also have increased the hardness of the as-received material, and none of this phase was observed in the solutioned (or in the solutioned + aged) material. Comparison of the data in figures 6 and 7 shows that the unreinforced matrix which was solutioned and aged at 300 °C/24 hr had a hardness that was 70 percent higher than that of the as-received coupon after aging at 300 °C/24 hr. This difference was probably the result of very fine, unresolvable α-particles which precipitated uniformly in the solutioned + aged material. Okada et al. (ref. 6) have shown that aging at 300 °C can produce a strong age-hardening condition due to the formation of small α-particles; however, this microstructure also exhibited brittle behavior. In contrast to the strong age-hardening behavior of the specimen given the 300 °C/24 hr heat treatment, the

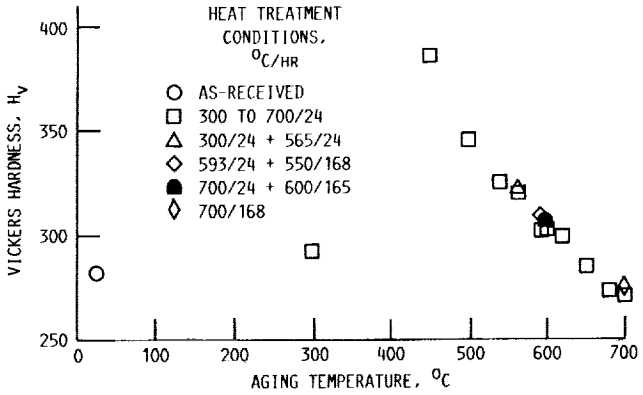

Figure 6.—Vickers hardness as function of aging condition for unreinforced matrix (Vickers hardness indentions made at 200-g load).

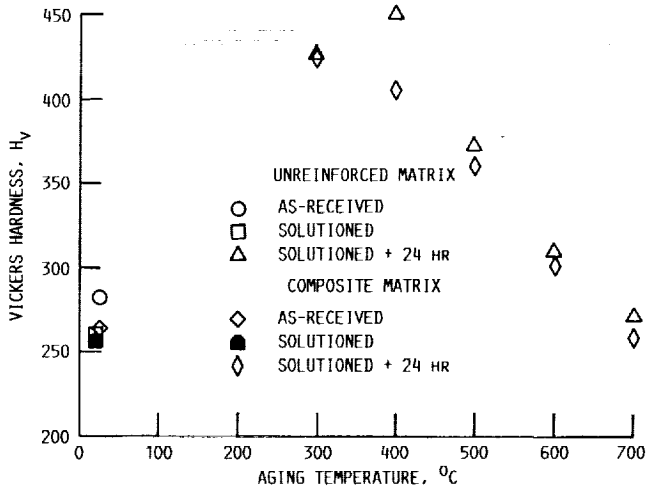

Figure 7.—Vickers hardness for unreinforced matrix and composite matrix in both solutioned and aged conditions (Vickers hardness indentions made at 200-g load).

coupon which was solutioned and aged at 700 °C for 24 hr had a low hardness, identical to that of the as-received coupon given a 700 °C/24 hr age. Figure 7 also indicates that the composite matrix after solutioning and after subsequent aging was consistently softer than the unreinforced matrix in the same condition. However, because of the inherent scatter in the measurement technique, these hardness values are statistically equivalent.

Hardness was similarly measured for the matrix in the heat-treated composite specimens, as depicted in figure 8. These values can be compared with those of the unreinforced matrix shown previously in figure 6. For hardness measurements of the precipitate lean zone surrounding the fibers, the indentation was placed as remote from the fiber as possible, yet still within the precipitate lean zone. Figure 8 shows that the hardness of the precipitate lean zone was consistently lower than elsewhere in the composite, but was statistically equivalent to that of the composite matrix. Apparently, the fibers cause local chemical inhomogeneities in the matrix.

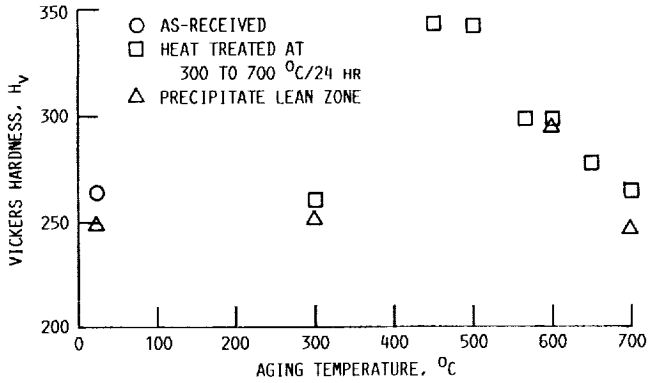

Figure 8.—Aging response of Vickers hardness for composite matrix (hardness of precipitate lean zone also included; Vickers hardness indentations made at 200-g load).

A microprobe trace between two fiber rows is shown in figure 9. These data are qualitative and show only relative changes in the composition. Figure 9 indicates that the silicon content was high near the fibers and decreased further into the matrix. Carbon shows the reverse trend, being highest halfway between fiber rows and lowest next to the fibers. Titanium, oxygen, and aluminum showed no large variation within the matrix. The reasons for the chemistry transients are unknown. Such differences in chemistry could cause a variation in the precipitate state within the matrix. Carbon has been shown in Ti-6Al-4V to be an α-stabilizer, and Si is typically a β-stabilizing element (ref. 13). Thus, α should have a tendency to precipitate in between fiber rows and have less of a tendency to precipitate near the fibers, which is indeed observed.

The hardness of the composite matrix was lower than that of the unreinforced matrix for both as-received and heat-treated materials. (Compare fig. 8 with fig. 6.) The peak aged condition occurs at ~450 °C for both materials, although the composite matrix had a peak hardness of 340 H_v compared with 385 H_v for the unreinforced matrix. At aging temperatures at or above 500 °C, this difference in hardness diminished. The difference in hardness at lower aging

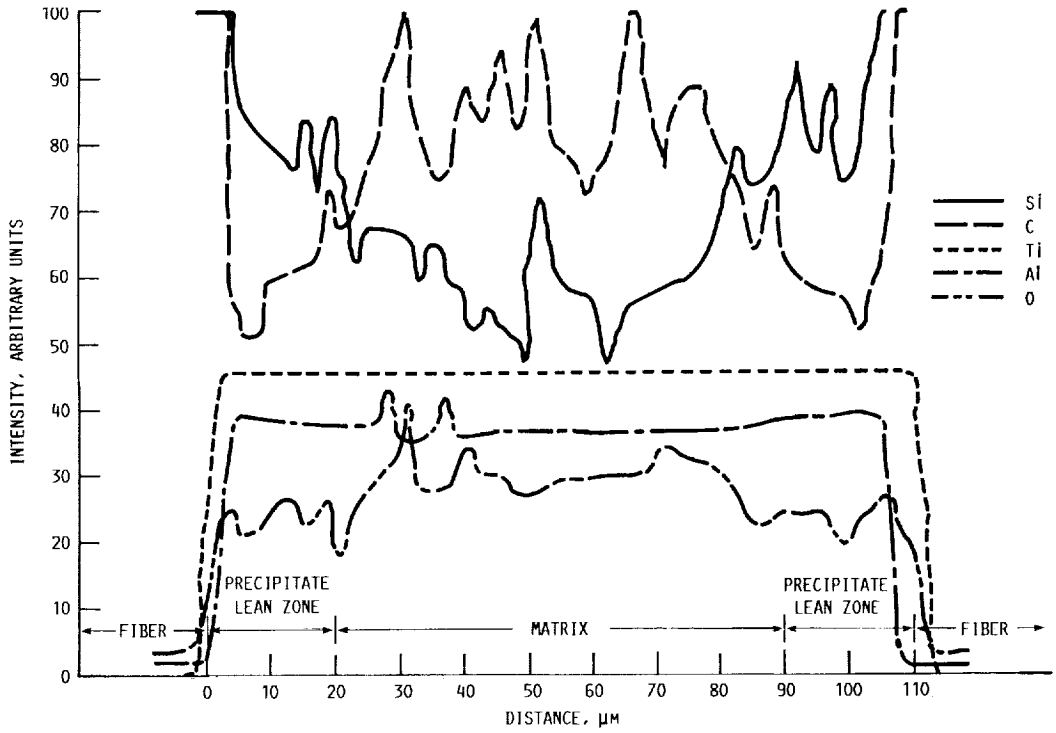

Figure 9.—Microprobe trace showing Si and C variations between two fiber rows (Si has maximum near fibers, whereas C peaks in matrix, between fiber rows).

temperatures could have been due to slightly different fabricating conditions. Therefore, both the unreinforced matrix and the composite were solutioned. Even after the solutioning, the composite matrix was softer than the unreinforced matrix (fig. 7), and generally the composite matrix remained softer than the unreinforced matrix after identical aging treatments. The unreinforced matrix peak hardened at 450 H_v after 24 hr at 400 °C, whereas the composite matrix peak hardened at 425 H_v after 24 hr at 300 °C. The slight difference in aging behavior is probably due to chemical variations as a result of the fiber additions, although other differences in chemistry between the two matrices could also have played a role.

It might be expected that fiber additions would alter the hardness of the matrix for several reasons. The differences in the coefficients of thermal expansion between the reinforcement and the matrix can cause residual stresses during the cooldown from consolidation. The stresses could be large enough to induce plasticity in the matrix. As such, the increase in dislocation density should work-harden the matrix, especially at the fiber/matrix interface where the stresses are highest. Vogelsang et al. (ref. 14) have shown transmission electron micrographs (TEM) of high dislocation densities surrounding the whisker and particulate reinforcements in aluminum. In the SiC/Ti-15-3 system, however, the in situ matrix is softer than the unreinforced matrix for a given aging condition. The influence of residual stresses on the microhardness of the in situ composite matrix is not yet fully characterized. Depending on the magnitude and direction, residual stresses may either increase or decrease the microhardness of the in situ composite material. Since the exact chemical composition controls the precipitation of α-phase, it can also affect the hardness of the in situ composite matrix. The micromechanics modeler should therefore be cautioned about using properties gained from testing the unreinforced matrix.

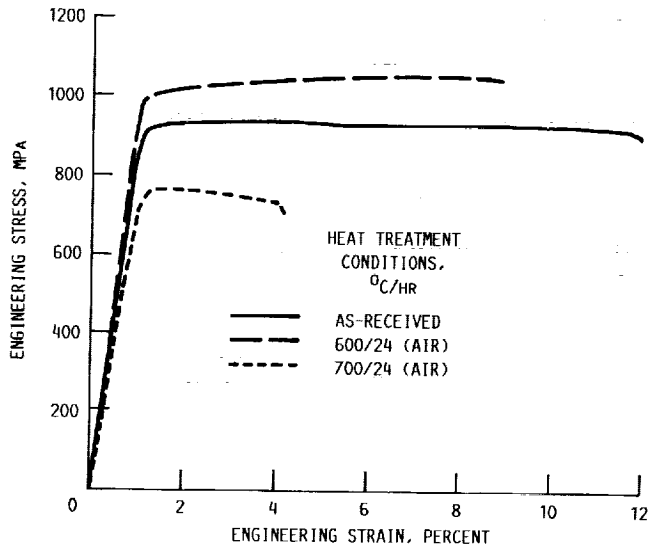

Figure 10.—Room-temperature stress-strain curves for unreinforced Ti-15-3 matrix.

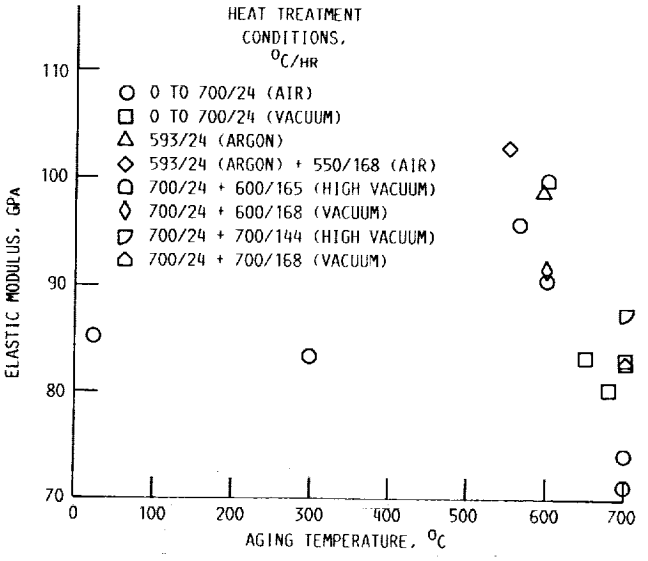

Figure 11.—Effect of aging on room-temperature elastic modulus of unreinforced matrix.

Mechanical Properties

Tensile specimens of the as-received, unreinforced matrix were aged and tested at room temperature to evaluate the effects of aging on the tensile properties. Because of a lack of material, similar tests were not performed on the composite. The stress-strain curves for the unreinforced matrix were similar in all cases in that little strain hardening was observed. (See fig. 10.) This is typical for many titanium alloys at room temperature (refs. 15 and 16). For micromechanics approaches, this material can be modeled as elastic, perfectly plastic. However, it should be cautioned that the in situ matrix may behave differently from the unreinforced matrix.

Figures 11 to 13 illustrate the tensile properties as a function of aging temperature. The values of elastic modulus were relatively constant at ~85 GPa after aging for 24 hr up to ~300 °C (fig. 11), whereas aging at 565 °C increased the elastic modulus to ~95 GPa. Aging at higher temperatures reduced the modulus considerably to a value of ~70 GPa after aging for 24 hr at 700 °C. This change in modulus as a function of heat treatment is unusually large compared to other metals, although it has been suggested (ref. 3) that the modulus of β-Ti alloys may change with heat treatment. Reportedly, β-Ti has a 16 percent lower modulus than α (ref. 13), but even if all the β transformed upon aging to α, this difference in modulus would not be sufficient to explain the changes observed in this study.

The ultimate tensile strength (UTS) is shown as a function of aging temperature in figure 12. A temperature dependence similar to that observed for elastic modulus can be seen. The UTS had a value of ~930 MPa after aging for 24 hr up to ~300 °C. After a 24 hr age at 565 °C, the tensile strength increased to ~1130 MPa. Aging at temperatures above 565 °C

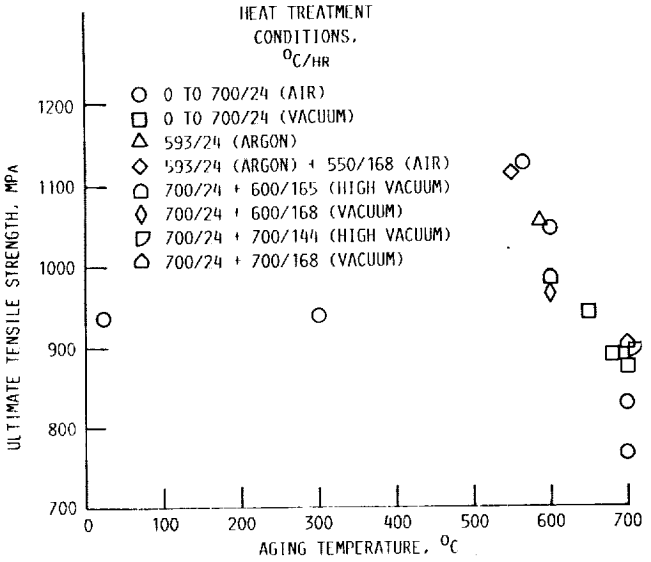

Figure 12.—Effect of aging on room-temperature ultimate tensile strength of unreinforced matrix.

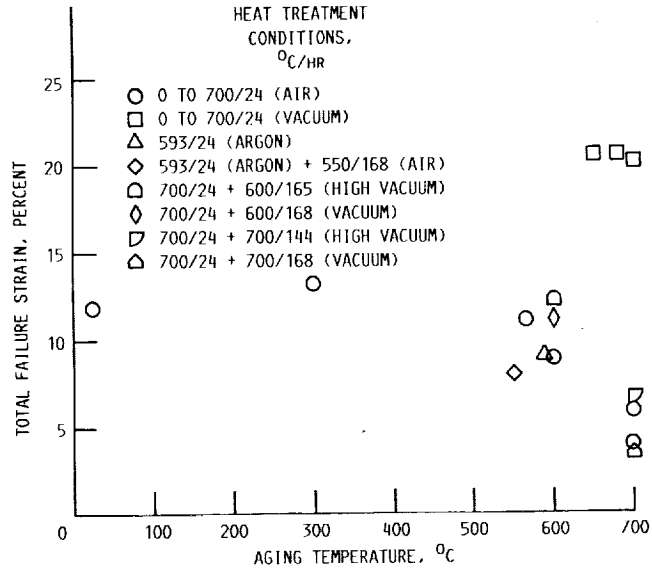

Figure 13.—Room-temperature failure strain as function of aging for unreinforced matrix.

lowered the tensile strength, with 750 MPa being the lowest UTS after an age of 24 hr at 700 °C. The response to aging of both the modulus and the UTS was identical to the response of the hardness. This included the duplex heat treatments (also represented in figs. 11 and 12), the final properties of which depended on the second step of the duplex heat treatment. A similar temperature dependence was also observed for the yield stress, but it will not be discussed here, since the yield stress was only slightly below the UTS (i.e., perfectly plastic response).

The ductility of the material, as represented by the failure strain, is presented in figure 13. The failure strain increased slightly at the aging temperature of 300 °C, and it decreased above 550 °C. However, specimens which were aged above ~550 °C in a vacuum exhibited extremely good ductility. Exceptions to this were the specimens given long-term exposures at 600 and 700 °C. Despite being heat treated in a vacuum, they had very low ductilities, probably a result of the large α-phase at laminae and grain boundaries. (See fig. 4.) Duerig and Williams (ref. 12) have found that the α-grain boundary phase is detrimental to ductility.

Summary of Results

The oxidation and aging characteristics of Ti-15-3 were studied. A comparison was made between the Ti-15-3 unreinforced matrix and the matrix within the SiC-reinforced Ti-15-3 composite. Optical microscopy, hardness, and tensile tests were used to evaluate the aging process in this material. The following points summarize the findings:

1. The Ti-15-3 must be protected from oxidation at temperatures greater than 550 °C to prevent the formation of a thick surface layer of oxide.

2. The hardness measurements of the unreinforced matrix and the in situ composite matrix both exhibited a peak as a function of aging temperature, with the maximum observed at ~450 °C for both materials. However, the in situ composite matrix was consistently softer than the unreinforced matrix in the as-received condition. The composite matrix remained softer than the unreinforced matrix even after additional aging treatments.

3. Chemical inhomogeneities introduced by the fibers resulted in a precipitate lean zone surrounding the fibers. Differences in matrix chemistry are suspected of causing the difference in aging behavior between the unreinforced matrix and the composite matrix.

4. The room-temperature elastic modulus and ultimate tensile strength of the unreinforced matrix are a function of the aging conditions, with a maximum observed after aging for 24 hr at a temperature between 350 and 550 °C.

5. An unusually large change in elastic modulus of the unreinforced matrix as a function of aging was observed.

6. The failure strain of the unreinforced matrix exhibited very small changes for aging temperatures up through 300 °C. Above 500 °C the ductility decreased. Aging at the higher temperatures in vacuum greatly increased the ductility, although long-term exposures to the higher temperatures (e.g., 600 and 700 °C) caused formation of large, grain boundary α which reduced the ductility.

Lewis Research Center
National Aeronautics and Space Administration
Cleveland, Ohio, August 1989

Appendix—Micrographs of Unreinforced Matrix and Composite for Various Heat Treatments

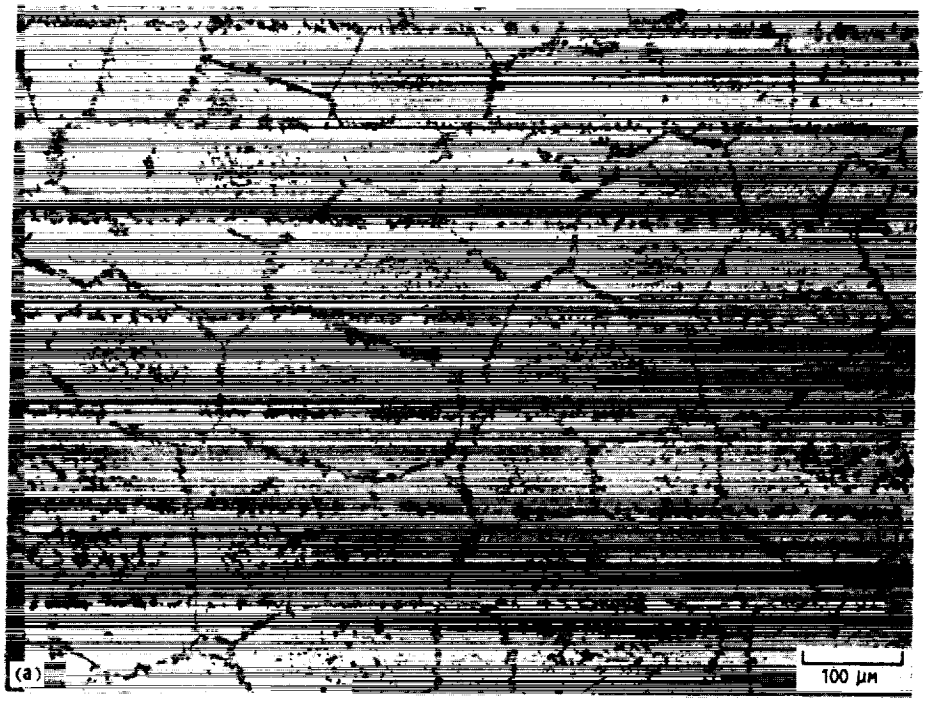

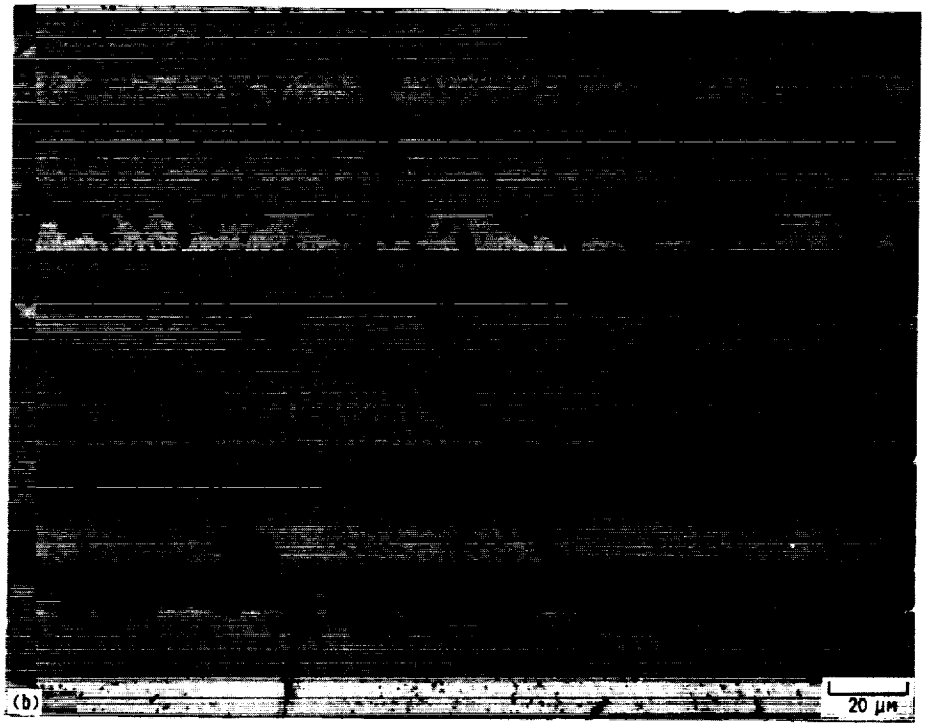

(a) Unreinforced matrix.
(b) Unreinforced matrix, enlarged view.

Figure 14.—As-received unreinforced matrix and composite matrix.

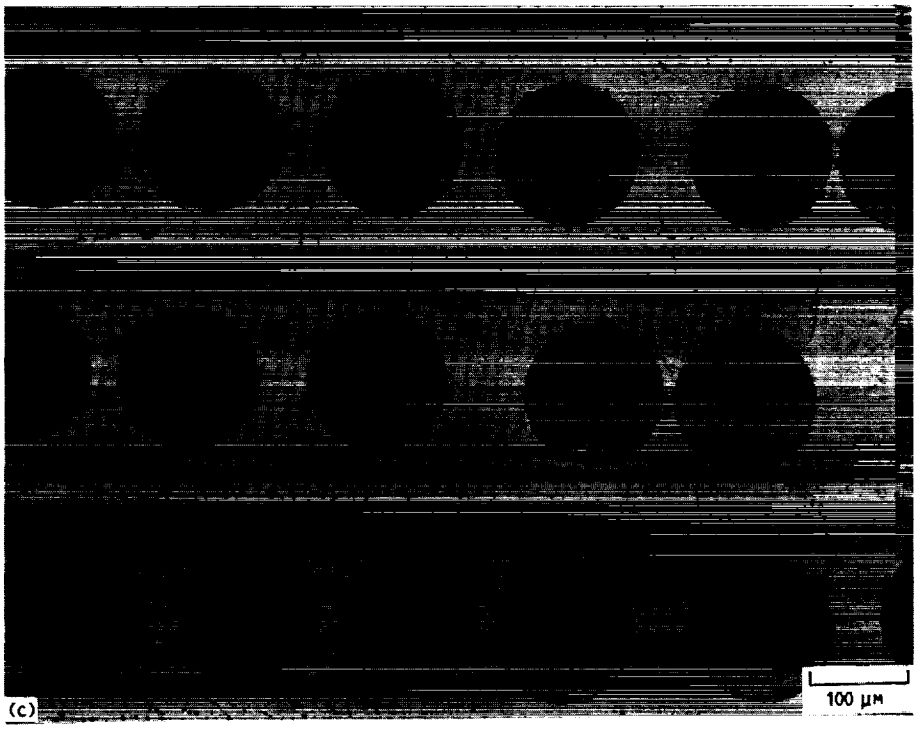

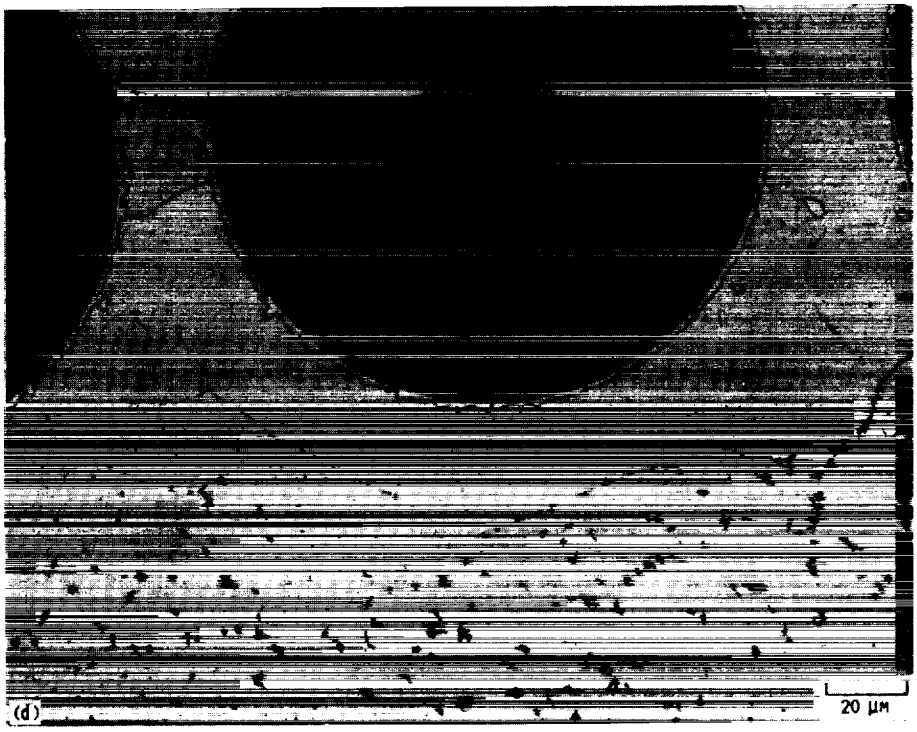

(c) Composite matrix.
(d) Composite matrix, enlarged view.

Figure 14.—Concluded.

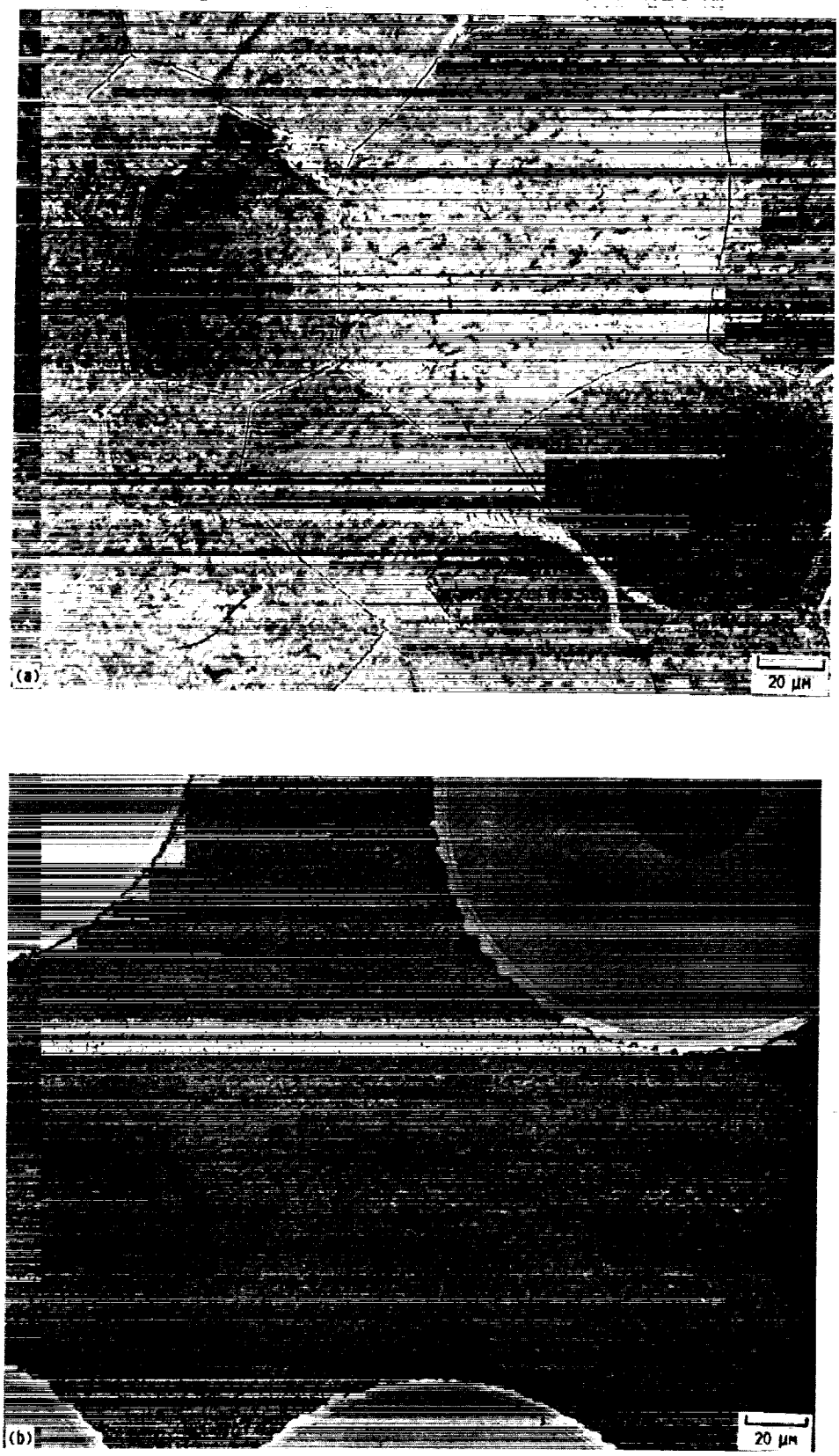

(a) Unreinforced matrix.
(b) Composite matrix.

Figure 15.—Unreinforced matrix and composite matrix after aging for 24 hr at 450 °C.

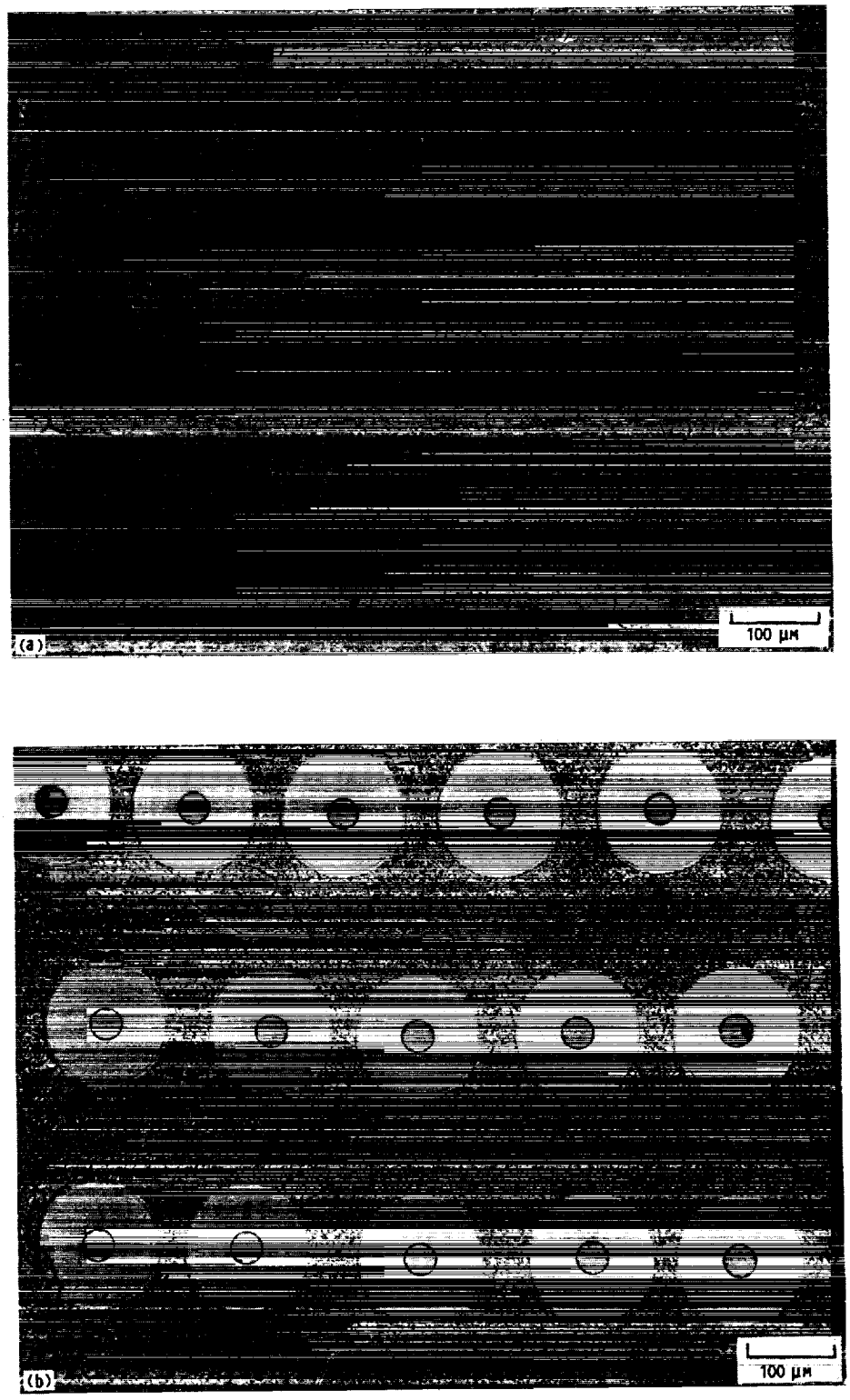

(a) Unreinforced matrix.
(b) Composite matrix.

Figure 16.—Unreinforced matrix and composite matrix after aging for 24 hr at 600 °C.

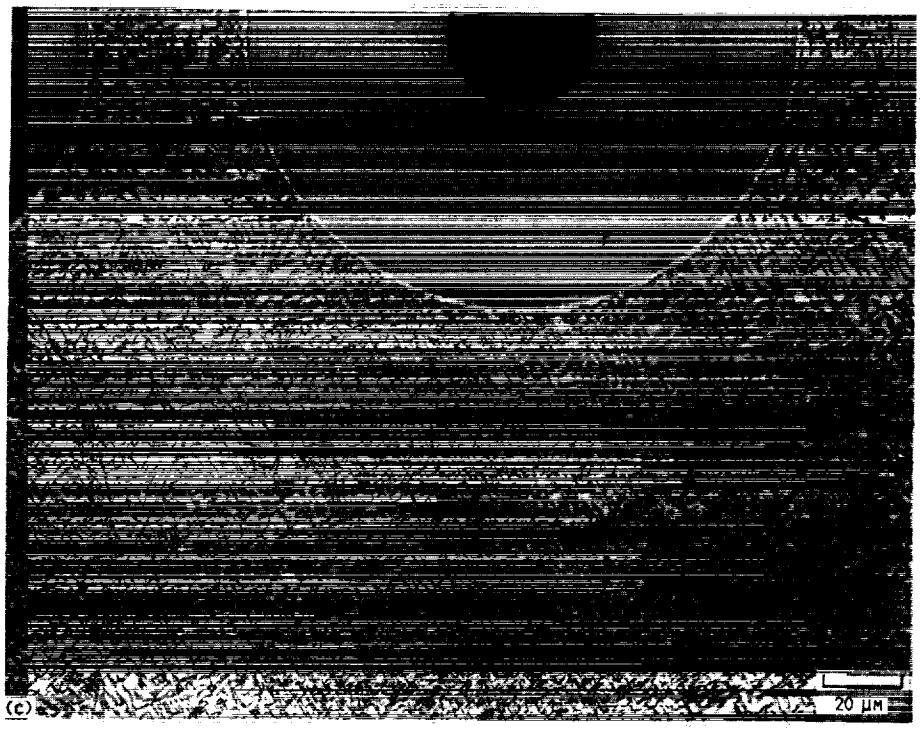

(c) Composite matrix, enlarged view.

Figure 16.—Concluded.

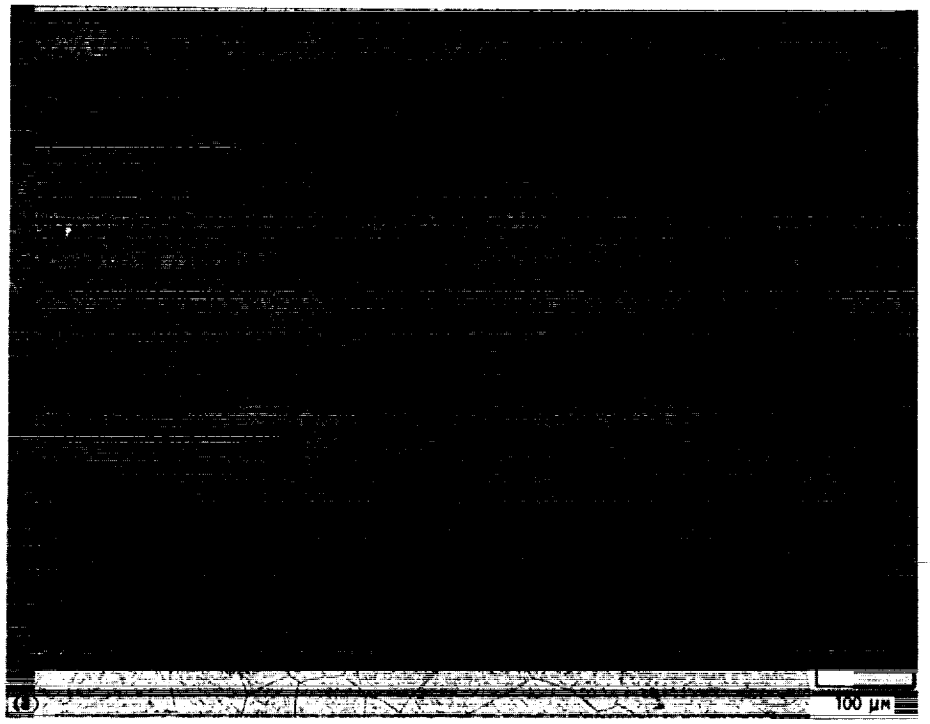

(a) Unreinforced matrix.

Figure 17.—Unreinforced matrix and composite matrix after aging for 24 hr at 700 °C.

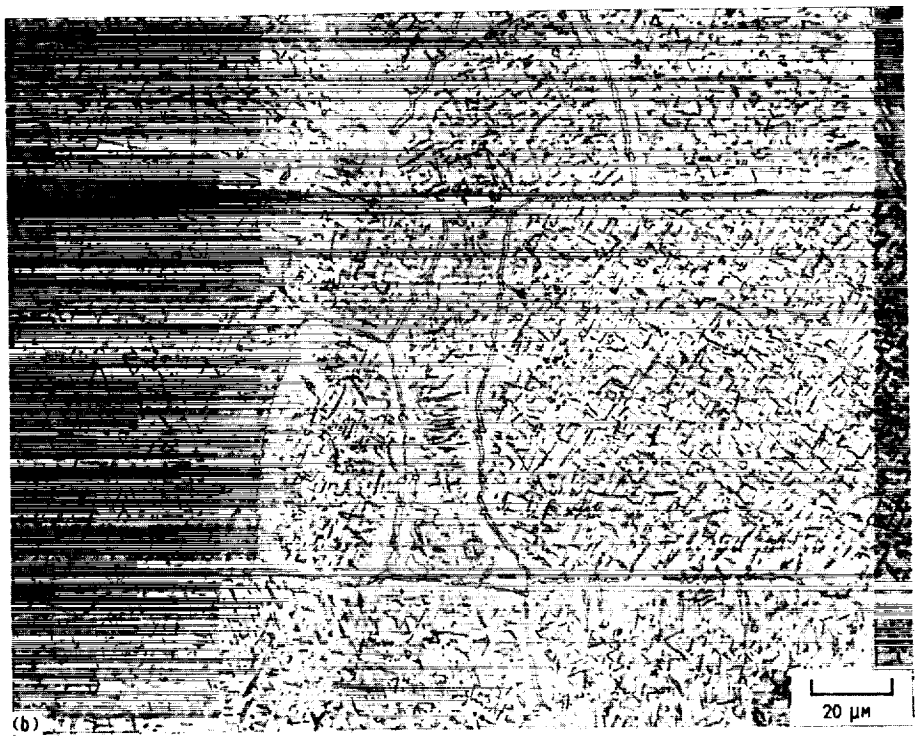

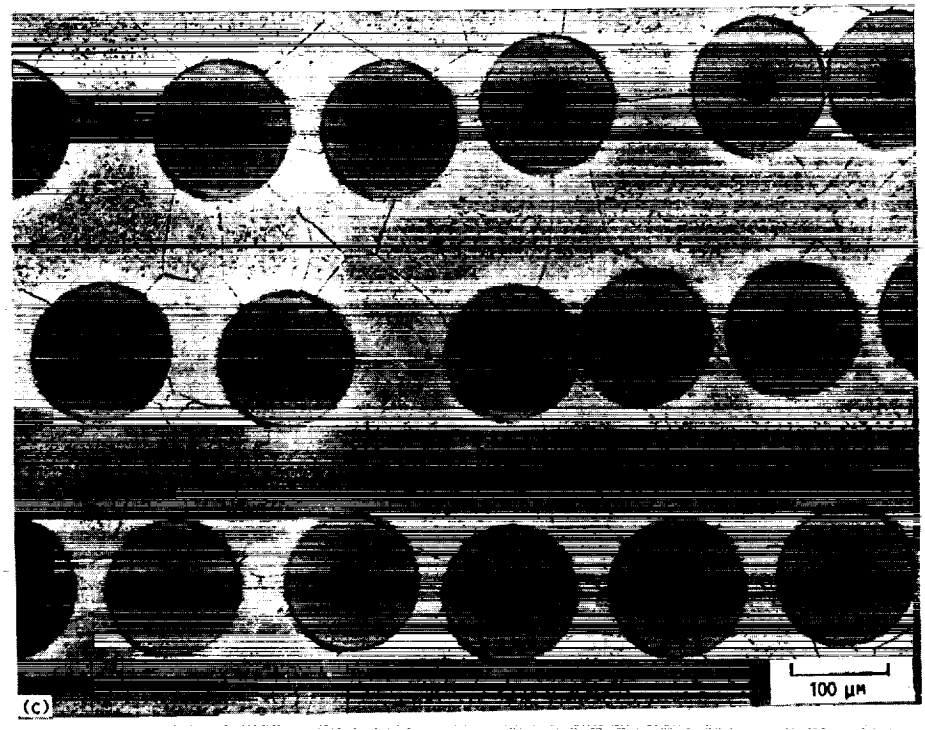

(b) Unreinforced matrix, enlarged view.
(c) Composite matrix

Figure 17.—Continued.

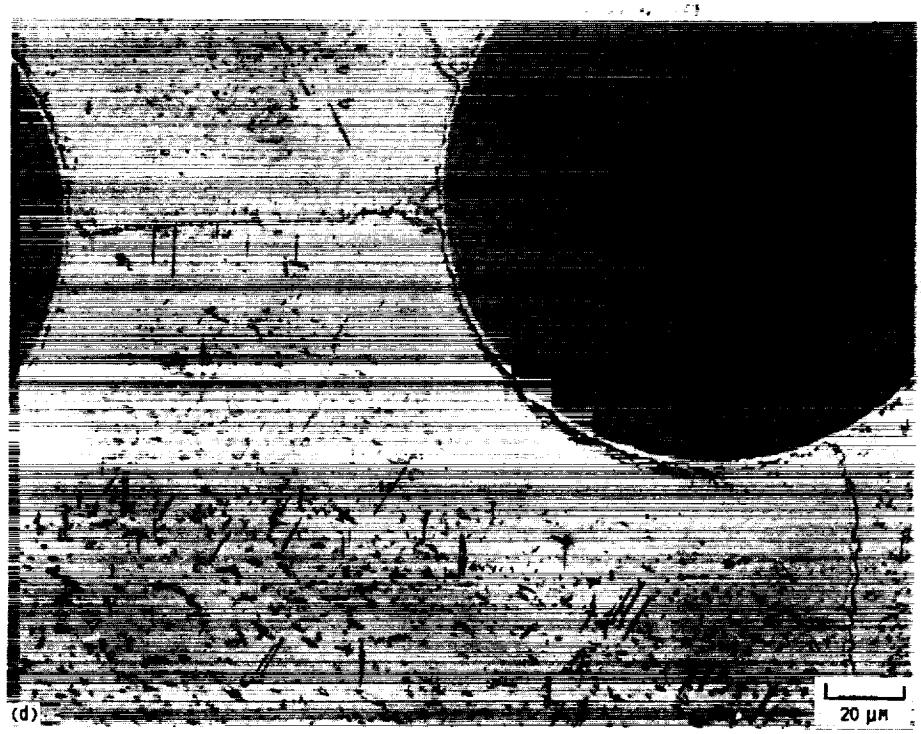

(d) Composite matrix, enlarged view.

Figure 17.—Concluded.

(a) Unreinforced matrix.

Figure 18.—Unreinforced matrix and composite matrix after aging for 24 hr at 700 °C, followed by aging for 165 hr at 600 °C.

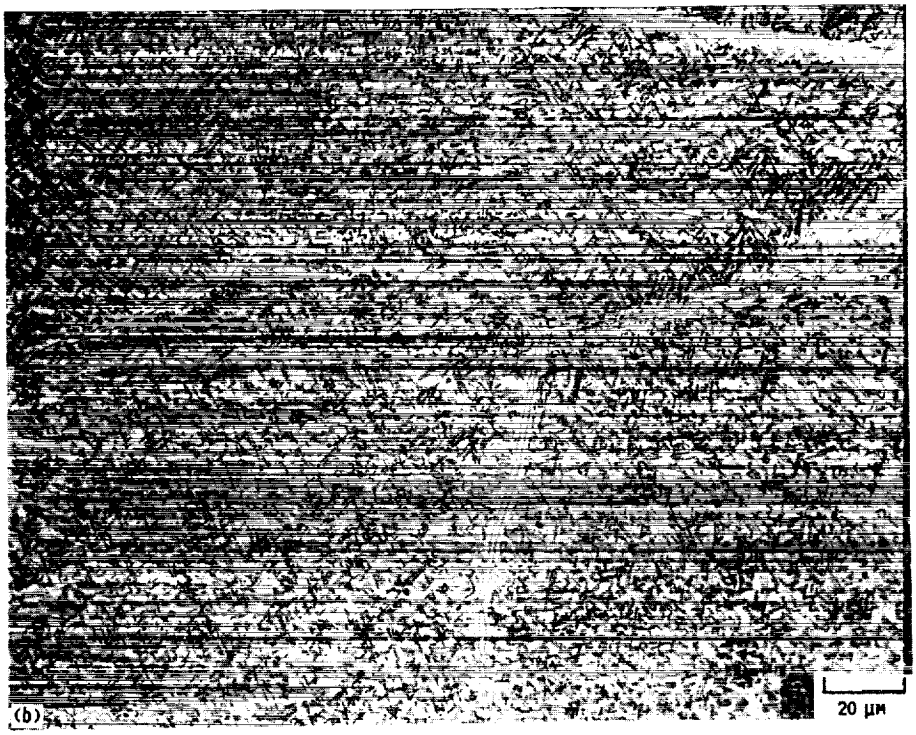

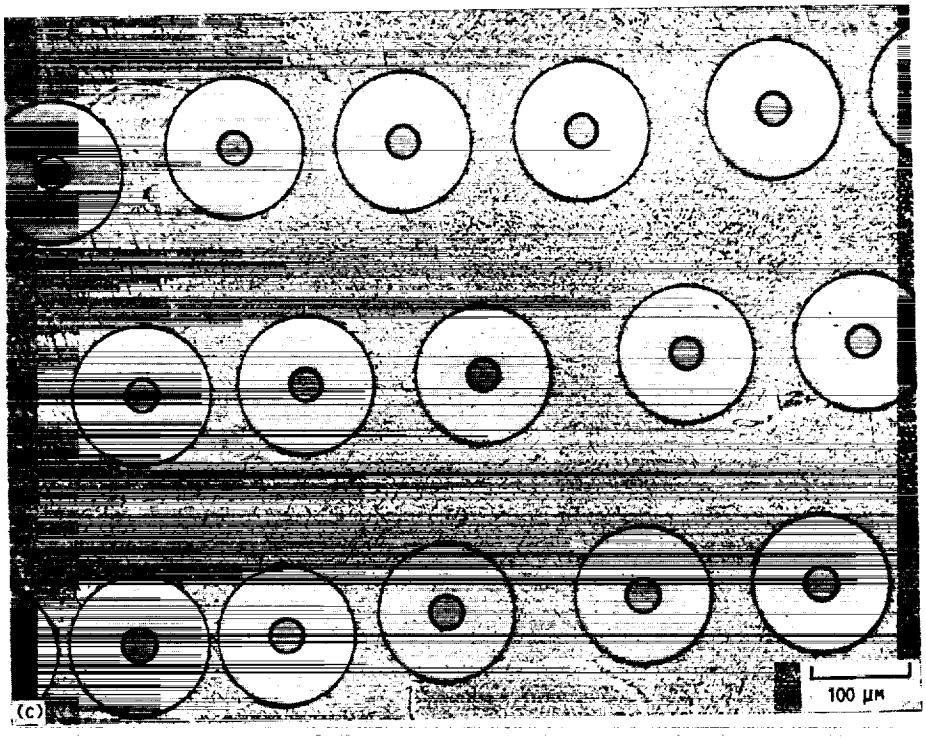

(b) Unreinforced matrix, enlarged view.
(c) Composite matrix.

Figure 18.—Continued.

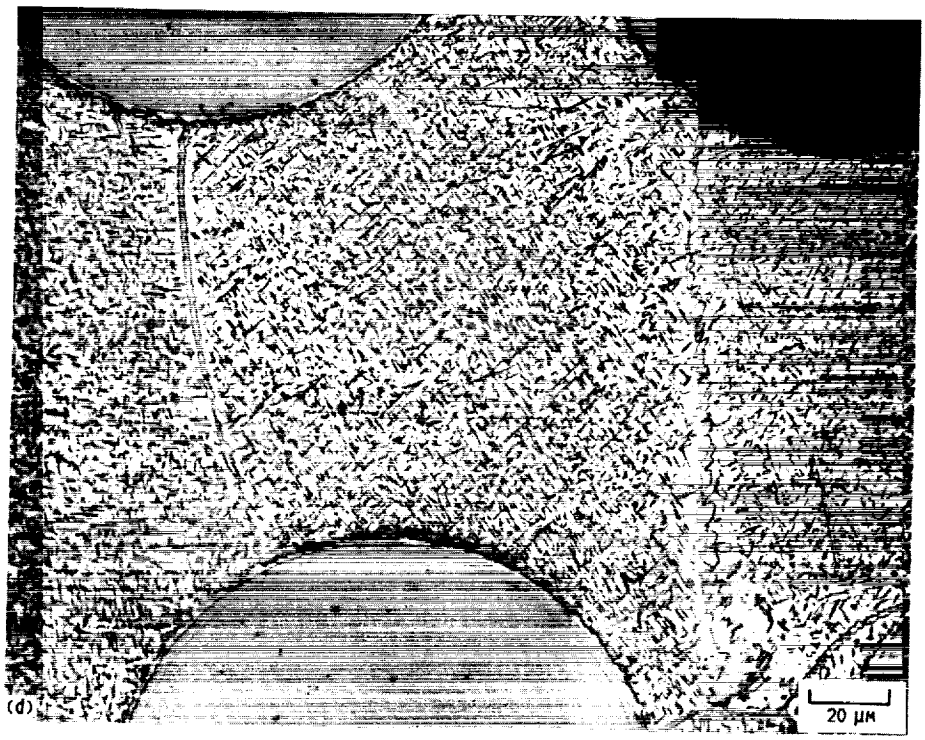

(d) Composite matrix, enlarged view.

Figure 18.—Concluded.

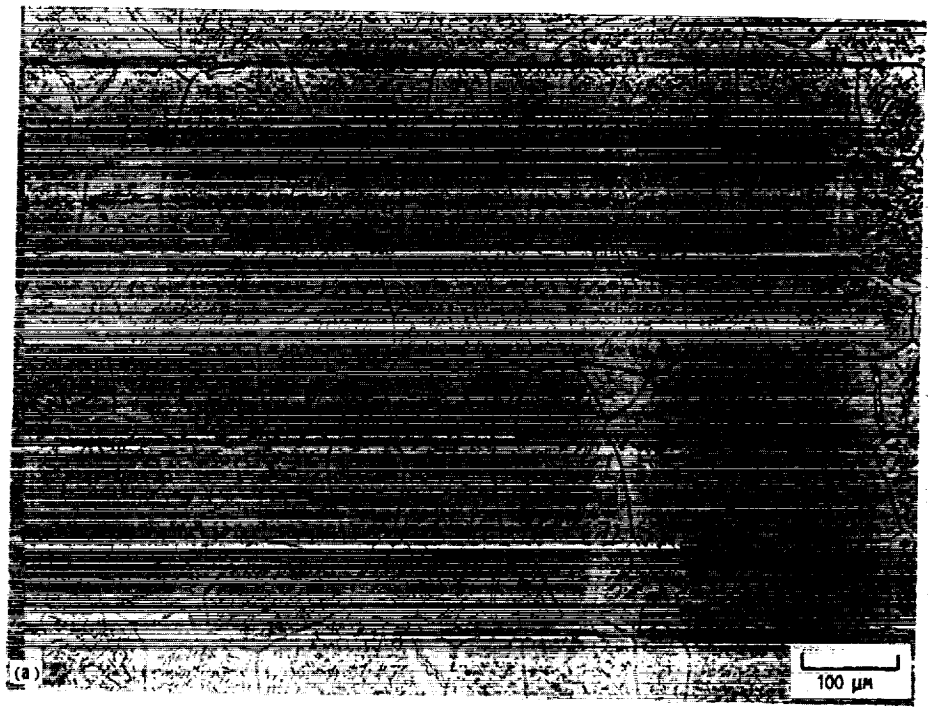

(a) Unreinforced matrix.

Figure 19.—Unreinforced matrix and composite matrix after aging for 168 hr at 700 °C.

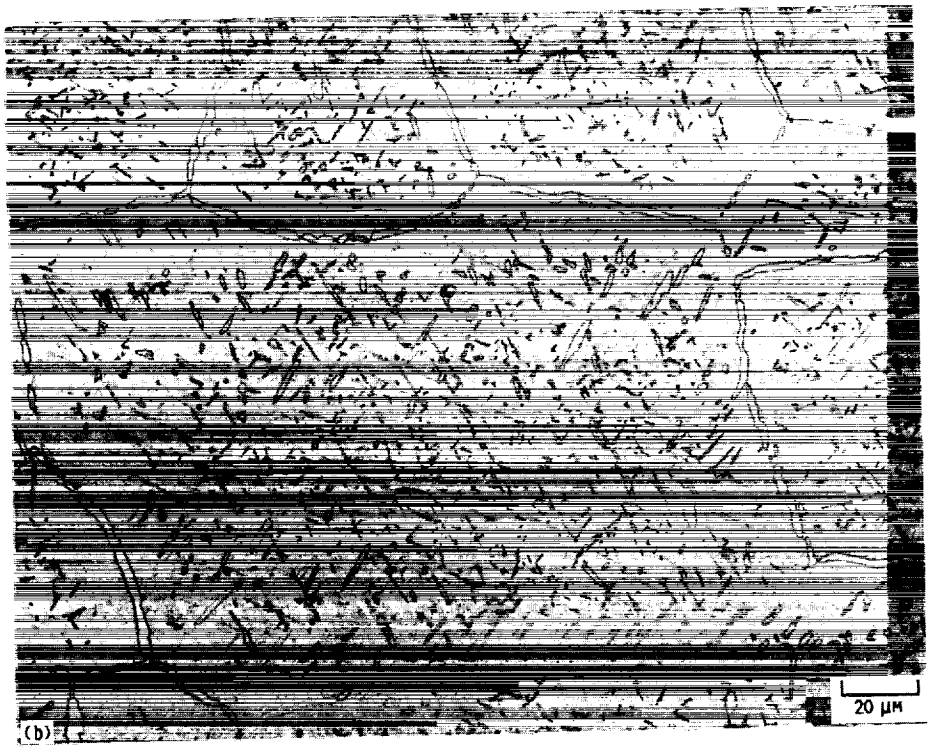

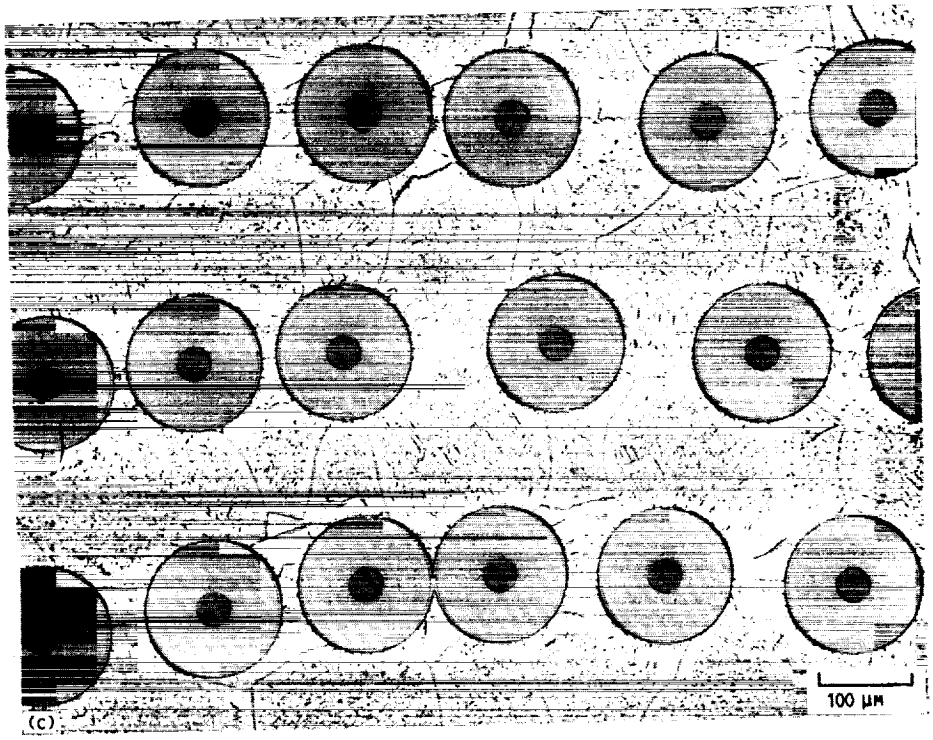

(b) Unreinforced matrix, enlarged view.
(c) Composite matrix.

Figure 19.—Continued.

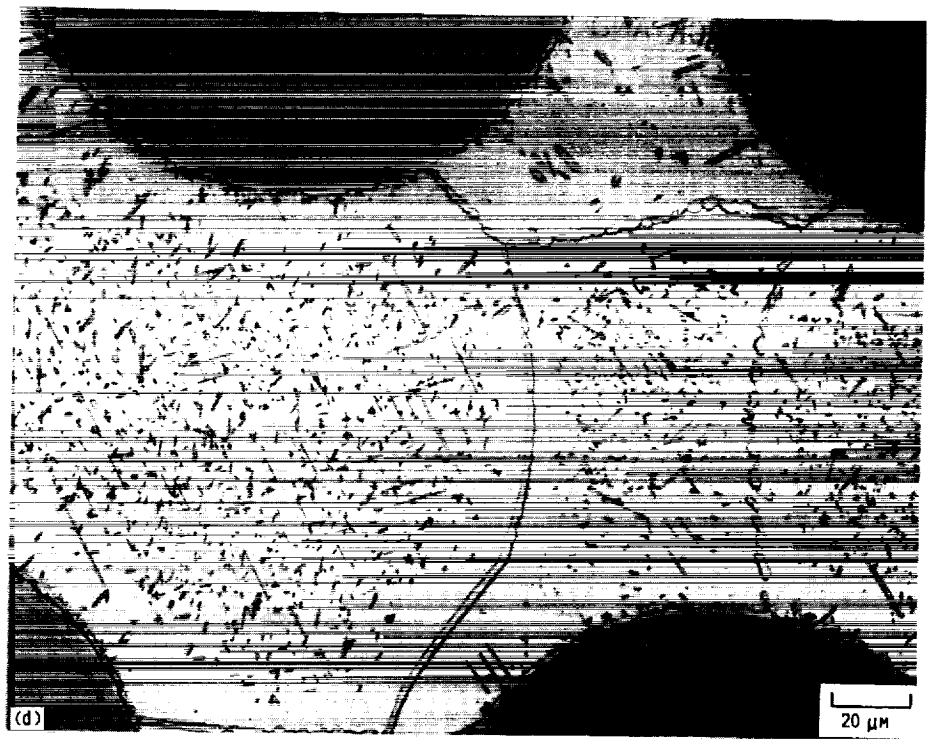

(d) Composite matrix, enlarged view.

Figure 19.—Concluded.

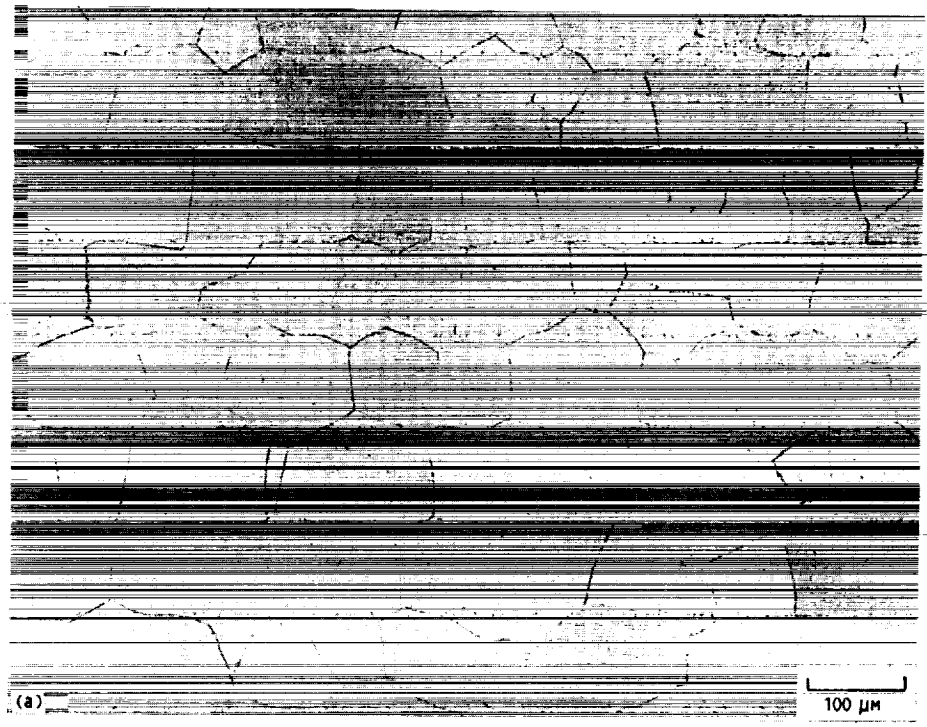

(a) Unreinforced matrix.

Figure 20.—Unreinforced matrix and composite matrix after solutioning for 0.25 hr at 788 °C, followed by a water quench.

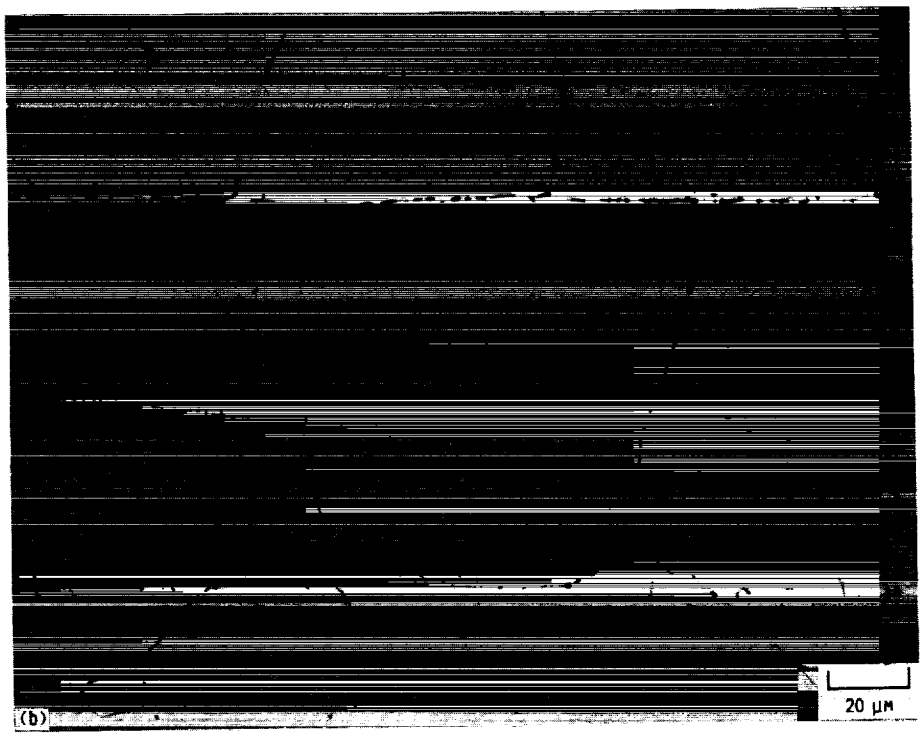

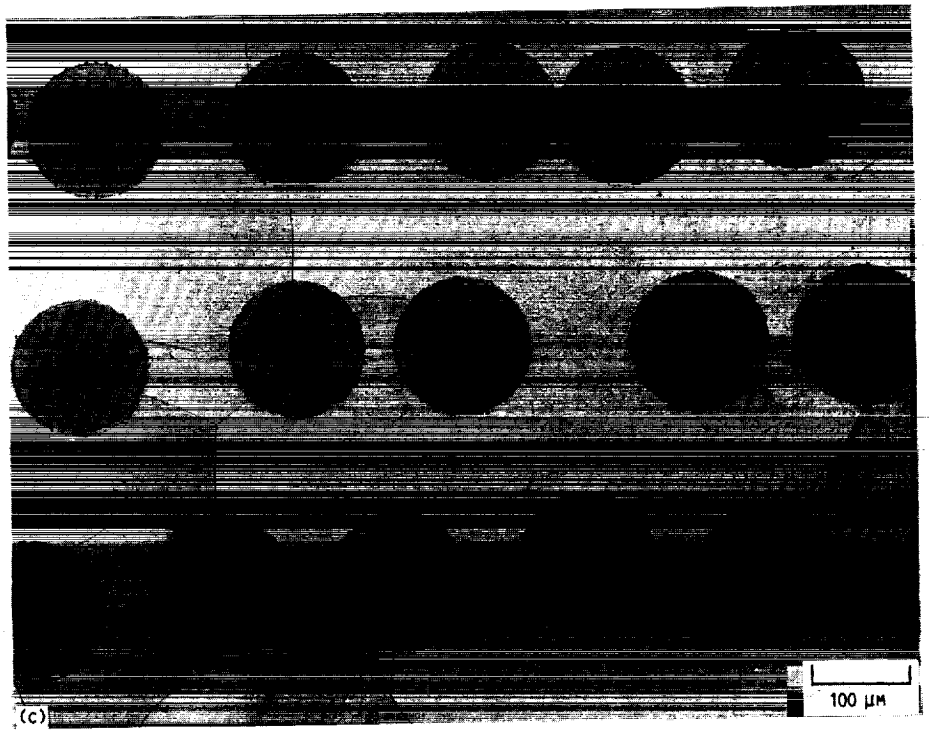

(b) Unreinforced matrix, enlarged view.
(c) Composite matrix.

Figure 20.—Concluded.

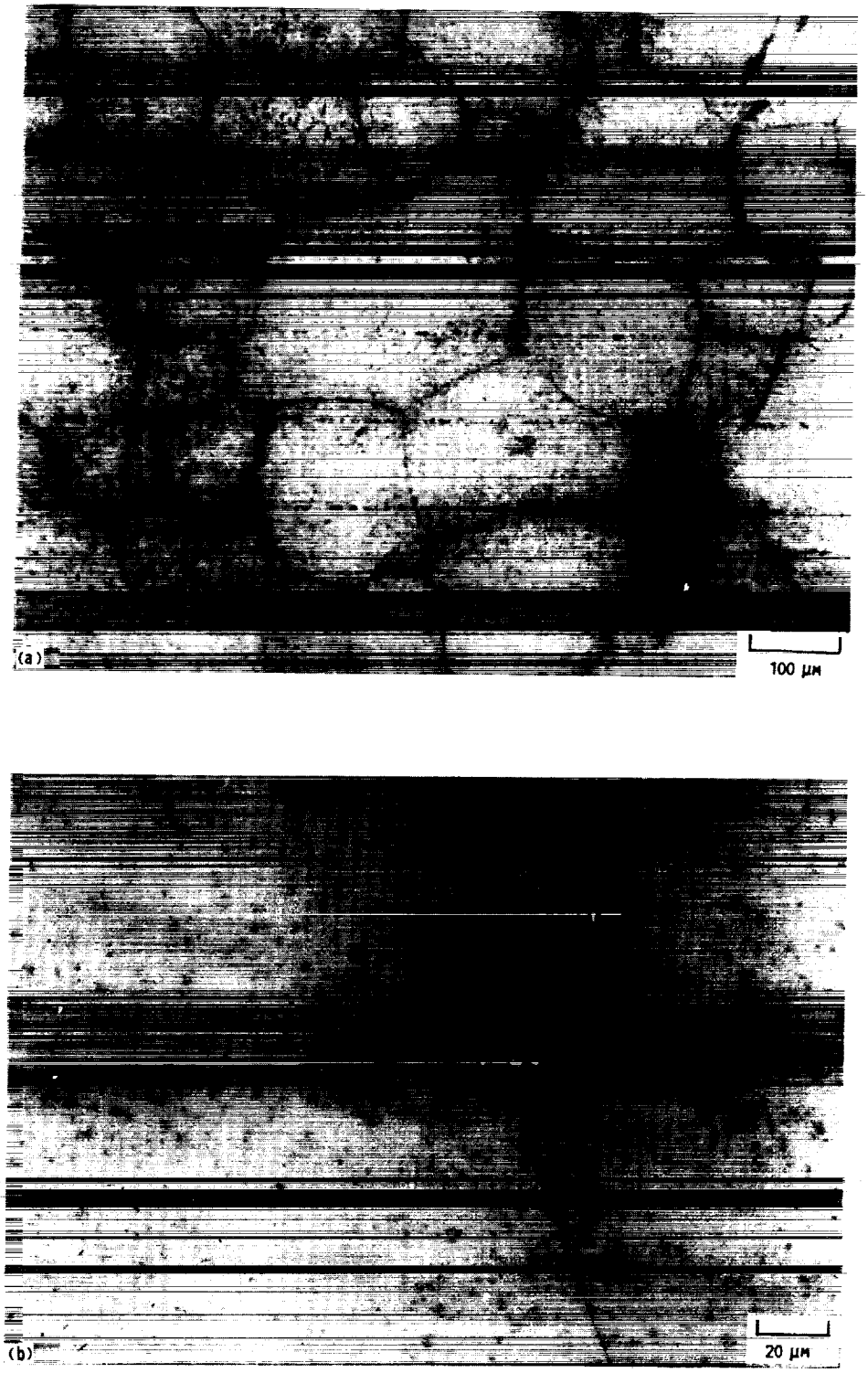

(a) Unreinforced matrix.
(b) Unreinforced matrix, enlarged view.

Figure 21.—Unreinforced matrix and composite matrix after solutioning for 0.25 hr at 788 °C, followed by a water quench and aging for 24 hr at 300 °C.

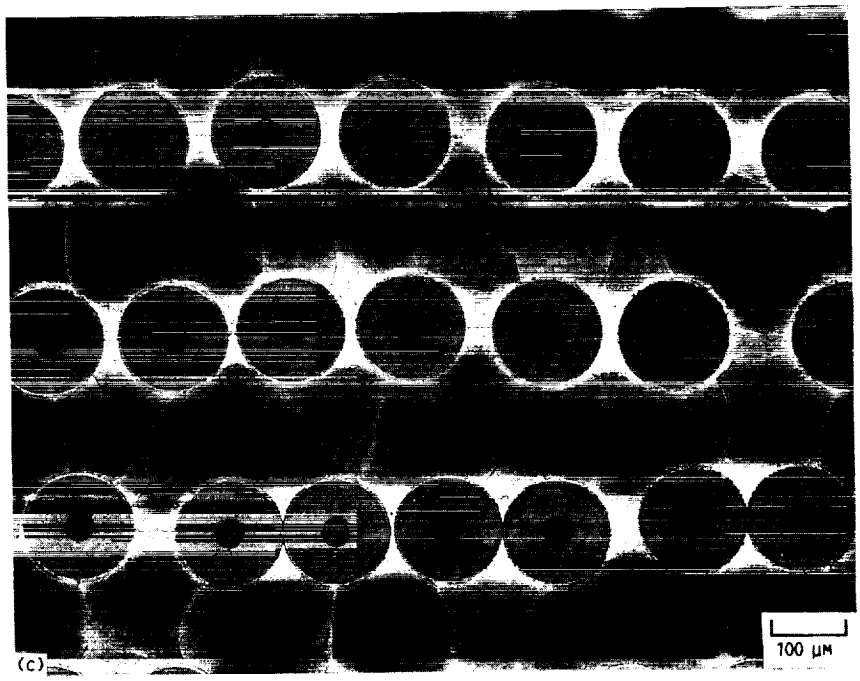

(c) Composite matrix.

Figure 21.—Concluded.

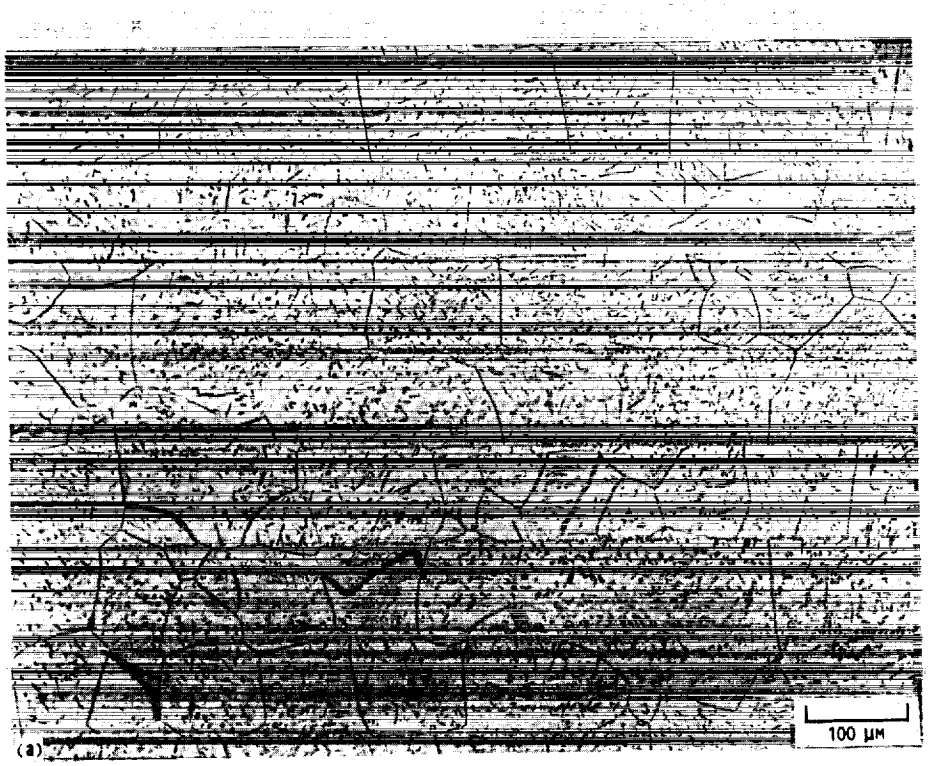

(a) Unreinforced matrix.

Figure 22.—Unreinforced matrix and composte matrix after solutioning for 0.25 hr at 788 °C, followed by a water quench and aging for 24 hr at 700 ° C.

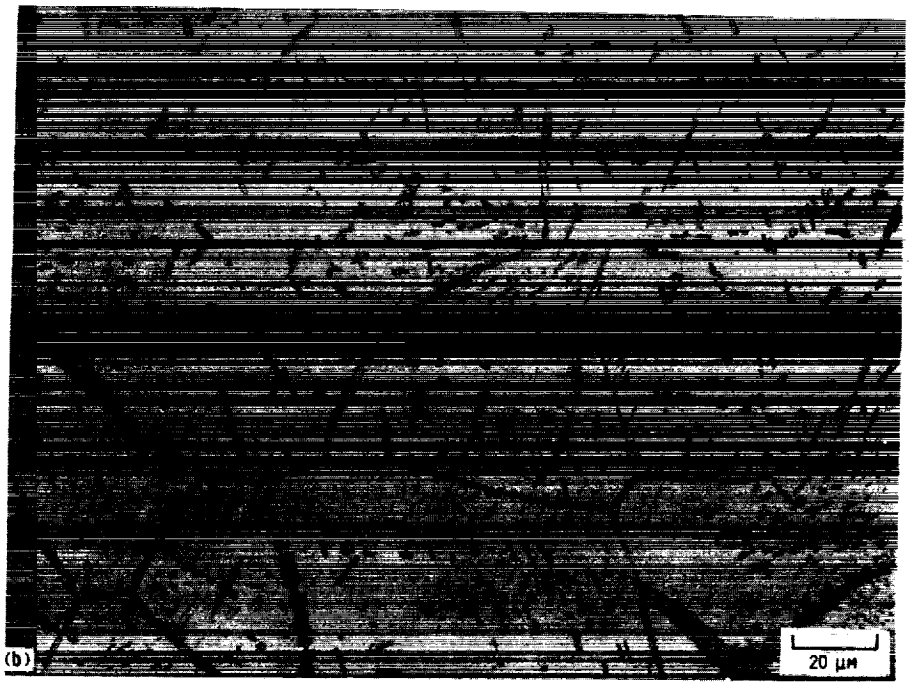

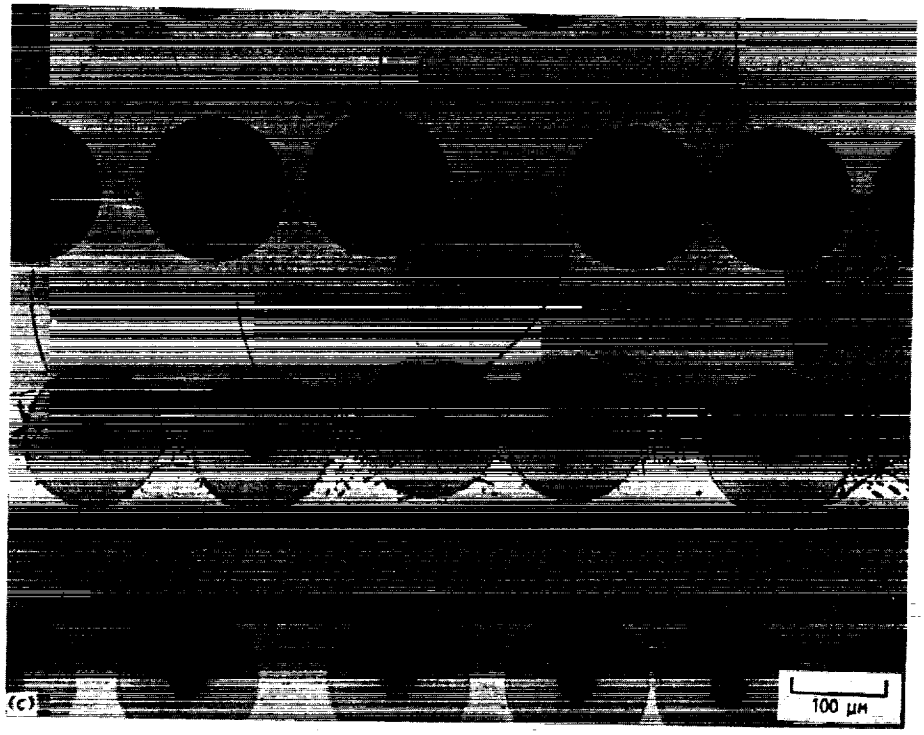

(b) Unreinforced matrix, enlarged view.
(c) Composite matrix.

Figure 22.—Continued.

(d) Composite matrix, enlarged view.

Figure 22.—Concluded.

References

1. Rosenberg, H.W.: Ti-15-3 Property Data. Beta Titanium Alloys in the 1980's, R.R. Boyer and H.W. Rosenberg, eds., TMS-AIME, Warrendale, PA, 1984, pp. 409-425.
2. Becker, D.W.; and Baeslack, W.A., III: Property-Microstructure Relationships in Metastable-Beta Titanium Alloy Weldments. Welding J., vol. 59, no. 3, Mar. 1980, pp. 85s-92s.
3. Metallic Materials and Elements for Aerospace Vehicle Structures. MIL-HDBK-5E, pp. 5.121-5.125.
4. Rosenberg, H.W.: Ti-15-3: A New Cold-Formable Sheet Titanium Alloy. J. Metals, vol. 35, no. 11, Nov. 1986, pp. 30-34.
5. Bania, P.J.; Lenning, G.A.; and Hall, J.A.: Development and Properties of Ti-15V-3Cr-3Sn-3Al (Ti-15-3). Beta Titanium Alloys in the 1980's, R.R. Boyer and H.W. Rosenberg, eds., TMS-AIME, Warrendale, PA, 1984, pp. 209-230.
6. Okada, M.; Banerjee, D.; and Williams, J.C.: Tensile Properties of Ti-15V-3Al-3Cr-3Sn Alloy. Titanium: Science and Technology, Vol. 3, G. Luetjering, U. Zwicker, and W. Bunk, eds., Deutsche Gesellschaft fuer Metallkunde, Oberursel, Federal Republic of Germany, 1985, pp. 1835-1842.
7. Ogden, H.R.; and Holden, F.C.: Metallography of Titanium Alloys. Titanium Metallurgical Laboratory, TML-103, Battelle Memorial Institute, Columbus, OH, 1958 (Avail. NTIS, AD-201292).
8. Lerch, B.A.; Hull, D.R.; and Leonhardt, T.A.: As-Received Microstructure of a SiC/Ti-15-3 Composite. NASA TM-100938, 1988.
9. Williams, J.C.: Critical Review Kinetics and Phase Transformations. Titanium Science and Technology, Vol. 3, R.I. Jaffee and H.M. Burte, eds., Plenum Press, 1973, pp. 1433-1494.
10. Ankem, S.; and Seagle, S.R.: Heat-Treatment of Metastable Beta-Titanium Alloys. Beta Titanium Alloys in the 1980's, R.R. Boyer and H.W. Rosenberg, eds., TMS-AIME, Warrendale, PA, 1984, pp. 107-126.
11. Rhodes, C.G.; and Paton, N.E.: The Influence of Microstructure on Mechanical Properties in Ti-3Al-8V-6Cr-4Mo-4Zr (Beta C). Metall. Trans. A, vol. 8, no. 11, Nov. 1977, pp. 1749-1761.
12. Duerig, T.W.; and Williams, J.C.: Overview: Microstructure and Properties of Beta-Titanium Alloys. Beta Titanium Alloys in the 1980's, R.R. Boyer and H W. Rosenberg, eds., TMS-AIME, Warrendale, PA, 1984, pp. 19-67.
13. Schmidt, F.F.; and Wood, R.A.: Heat Treatment of Titanium and Titanium Alloys. NASA TM X-53445, 1966.
14. Vogelsang, M.; Arsenault, R.J.; and Fisher, R.M: An In Situ HVEM Study of Dislocation Generation at Al/SiC Interfaces in Metal Matrix Composites. Metall. Trans. A, vol. 17, no. 3, Mar. 1986, pp. 379-389.
15. Rosenberg, H.W.: Stress-Strain Curves in Alpha Ti Alloys—Some Problems and Results. Metall. Trans. A, vol 8, no. 3, Mar. 1977, pp. 451-455.
16. Aerospace Structural Metals Handbook. Metals and Ceramics Information Center, Battelle Laboratories, Columbus. OH, 1989.

NASA
National Aeronautics and Space Administration

Report Documentation Page

1. Report No.	2. Government Accession No.	3. Recipient's Catalog No.
NASA TP-2970		

4. Title and Subtitle	5. Report Date
Heat Treatment Study of the SiC/Ti-15-3 Composite System	January 1990
	6. Performing Organization Code

7. Author(s)	8. Performing Organization Report No.
Bradley A. Lerch, Timothy P. Gabb, and Rebecca A. MacKay	E-4985
	10. Work Unit No. 510-01-01

9. Performing Organization Name and Address	11. Contract or Grant No.
National Aeronautics and Space Administration Lewis Research Center Cleveland, Ohio 44135-3191	
	13. Type of Report and Period Covered: Technical Paper

12. Sponsoring Agency Name and Address	14. Sponsoring Agency Code
National Aeronautics and Space Administration Washington, D.C. 20546-0001	

15. Supplementary Notes

16. Abstract

The oxidation and aging behaviors of a continuous fiber SiC/Ti-15V-3Cr-3Sn-3Al composite (SiC/Ti-15-3) were investigated. The aging characteristics of the composite were compared with those of the unreinforced Ti-15-3 matrix material, which was processed in the same manner as the composite. Various age-hardened conditions of both the unreinforced matrix and the composite were evaluated by using optical microscopy, hardness measurements, and room-temperature tensile tests (unreinforced matrix only). The Ti-15-3 material formed a thick surface oxide at temperatures at or above 550 °C when heat treated in air. The in situ composite matrix was softer than the unreinforced matrix for equivalent aging conditions. Both materials hardened to a maximum, then softened during overaging. The temperature at which peak aging occurred was ~450 °C for both the in situ composite matrix and the unreinforced matrix. The room-temperature elastic modulus and ultimate tensile strength of the unreinforced matrix varied as a function of aging treatment and paralleled the hardness behavior. The modulus and tensile strength showed little response to aging up to temperatures of 300 °C; however, these properties increased after aging at 550 °C. Aging at temperatures above 550 °C resulted in a decrease in the modulus and tensile strength. The failure strain was a function of the precipitation state and of the amount of oxidation resulting from the heat treatment. Aging in air at the higher temperatures (>550 °C) caused the formation of a thick oxide layer and reduced the ductility. Aging in vacuum at these temperatures resulted in significantly higher ductilities. Long-term exposures at 700 °C caused the formation of a large, grain boundary α-phase which reduced the ductility, even though the specimens were heat treated in vacuum.

17. Key Words (Suggested by Author(s))	18. Distribution Statement
Ti-SiC; Ti-15-3; Composite metallography; SiC/Ti; Aging Study; Heat treatment	Unclassified – Unlimited Subject Category 24

19. Security Classif. (of this report)	20. Security Classif. (of this page)	21. No of pages	22. Price*
Unclassified	Unclassified	30	A03

NASA FORM 1626 OCT 86

*For sale by the National Technical Information Service, Springfield, Virginia 22161

NASA-Langley, 1990